Seismic Evaluation and Retrofitting of an Existing Buildings-State of the Art

Haider Ali Abass [1], Husain Khalaf Jarallah [2*]

Author's affiliations:

1) Dept. of Civil Eng., Mustansiriyah University, Baghdad-Iraq.
hiaderaabass@uomustansiriyah.edu.iq

2*) Dept. of Civil Eng., Mustansiriyah University, Baghdad-Iraq.
khalfdce@uomustansiriyah.edu.iq

Abstract

In this study, previous researches were reviewed in relation to the seismic evaluation and retrofitting of an existing building. In recent years, a considerable number of researches has been undertaken to determine the performance of buildings during the seismic events. Performance based seismic design is a modern approach to earthquake resistant design of reinforcement concrete buildings. Performance based design of building structures requires rigorous non-linear static analysis. In general, nonlinear static analysis or pushover analysis was conducted as an efficient instrument for performance-based design. Pushover analysis came into practice after 1970 year. During the seismic event, a nonlinear static analysis or pushover analysis is used to analyze building under gravity loads and monotonically increasing lateral forces. These building were evaluated until a target displacement reached. Pushover analysis provides a better understanding of buildings seismic performance, also it traces the progression of damage and failure of structural components of buildings.

Keywords: Seismic Evaluation, Pushover Analysis, Seismic Retrofitting, Performance Based Design.

<div dir="rtl">

التقييم الزلزالي و التحديث للمباني القائمة-التطور الزمني للادبيات

حيدر علي عباس ، حسين خلف جارالله

الخلاصة:

في هذه الدراسة، تم مراجعة الأبحاث السابقة فيما يتعلق بالتقييم الزلزالي والتقوية لمباني قائمة. في السنوات الأخيرة ، تم إجراء عدد كبير من الأبحاث لتحديد أداء المباني خلال الاحداث الزلزالية. التصميم الزلزالي القائم على الأداء هو نهج حديث للتصميم المقاوم للزلازل للمباني المكونة من الخرسانة المسلحة. يتطلب التصميم القائم على الأداء الانشائي للمباني تحليلا" لا خطي دقيق. بشكل عام ، يتم إجراء التحليل السكوني غير الخطي أو الاختبار المبسط Pushover Test كأداة فعالة للتصميم المستند على الأداء. دخل الاختبار المبسط Pushover Test حيز التنفيذ بعد عام 1970 خلال الحدث الزلزالي, تستعمل طريقة الاختبار المبسط Pushover Test لتحليل الابنية تحت أحمال الجاذبية والقوى الجانبية المتزايدة بشكل رتيب. يتم تقييم هذه الابنية حتى يتم الوصول إلى الازاحة المستهدفة. يوفر الاختبار المبسط Pushover Test فهماً أفضل لاداء المباني الزلزالي ويتتبع أيضًا تطور الضرر وفشل المكونات الانشائية للمباني.

</div>

1. Introduction

Buildings are usually designed for seismic resistance using elastic analysis, most of which experiences significant inelastic deformations under large seismic events. Modern performance-based design methods require ways to define the real behavior of structures under such conditions. Non-linear analysis can show an important role in the design of new and existing buildings [1]. This review will effort on recent contributions associated with seismic evaluation and past attempts most closely associated with the seismic evaluation and retrofitting of an existing building. With the improvement of computational techniques, more difficult methods of seismic evaluation have been

recommended. Analytical methods can be carried out in absence of past earthquake damage records for a like type of buildings. It is also used to evaluate an individual building or type of buildings that has the same structural characteristics. Based on those facts, analytical approaches have been used to evaluate the seismic resistance of existing buildings. The Capacity Spectrum Method (CSM), A method for capturing the performance point provides a graphical statement of the structure's global force-displacement capacity curve and compares it to the response spectra representation of the demands of earthquakes. The inelastic capacity of a building is then calculating of its capability to scatter earthquake energy [2]. The Displacement Coefficient Method

(DCM) affords a direct numerical process for calculating the displacement demand. It is based on changing the linear elastic response of the SDOF system by developing it by chains of the coefficients to the nonlinear inelastic response of the MDOF system [3]. The outlines of this study included a review and discussion of the seismic assessment codes, a review of previous studies related to the pushover analysis, procedures for torsional effects, and a discussion of better ways to retrofit the existing buildings. The aim of this study is to indicate that the pushover method is an effective tool for evaluating and rehabilitation the existing building.

2. Methodology for Performance Evaluation
2.1 Structural damage parameters
The choice of appropriate damage parameters is very important for performance evaluation. Overall lateral deflection, inter-story drift and plastic hinge rotation are the most usually used damage parameters. Overall defection is not always a good indicator of damage, but the inter-Story drift is quite helpful because it is typical of the damage to the lateral load resisting system. Also, the maximum values of a member or joint rotations, curvature, and ductility factors are good guides of damage because they can be directly associated with the element deformation capacities. However, the maximum value alone of any of these parameters may not be sufficient to measure the overall damage caused by a cyclic reversal of deformation. Damage indicates which take into account both the maximum deformation and cyclic effects have been grown for such cases. Both indices can be used to calculate the overall damage state of a structure [4].

2.2 Displacement based damage parameters
The vulnerability of many existing structures may be the reason for structural weaknesses and low ductility. Common weaknesses in the structural system are due to lake in the load-path, strength and stiffness discontinuities, (vertical, horizontal, and mass) irregularities, weak column and strong beam, and eccentricities. Low ductility detailing is considered as insufficient shear reinforcement, inadequate confinement, and lacking anchorage length of the beam-reinforcement bars [5]. Commonly used displacement-based damage parameters are lateral drift or roof displacement; inter story drift, member or joints rotations, curvature and ductility factors, etc. Lateral drift and inter-Story drift are very commonly used parameters and are part of the direct output of performance level. Inter-story drift or Inter-Story drift ratio (IDR), defined as the comparative translational displacement between two consecutive floors divided by the story height is an important engineering response amount and indicator of structural performance. It shows an important role in determining the level of damage to columns during lateral deformation. Inter-story drift can also be used as a calculate of non-structural damage. Although the maximum values of the displacement-based damage parameters offer a good measure of damage, it does not account for the damage caused by a cyclic reversal of deformation that happens during earthquakes. Various energy-based damage parameters are available [6].

2.3 Review of Displacement based damage parameters
Biddah et al. [7] found that the inter-story drift does not account for accumulative damage because of repeated inelastic deformation. Also, the relationship between damage and inter-story drift different relying on the maximum deformation at collapse which depends on the ductility category of the structure.

Ghobarah [8] found that the inter-story drift is associated with different damage levels of different reinforced concrete components. Two main groups of drift limits were defined for ductile and non-ductile structural systems. In ductile structural system case, the relationship between the roof drift and the maximum inter-story drift is linear with a 45° slope. For existing non-ductile structures and poorly designed frames, the maximum inter-story drift of the soft story may show collapse while the roof drift will equal to a lower damage level.

Erduran and Yakut. [9] observed that the most important parameters affecting the damageability of RC columns are the yield strength of longitudinal reinforcement, the slenderness of the column and level of confinement.

2.4 Energy-based damage parameters
2.4.1 Energy dissipation by a structure
It is necessary to assess accurately the cyclic behavior of structural members which is illustrated by three primary ingredients: strength, deformability, and energy dissipation capacity (per load cycle). Commonly, reinforced concrete members show compound cyclic behavior with stiffness degradation. Therefore, the evaluation of the seismic performance of RC members is usually restricted to strength and deformability [10]. The estimation of energy dissipation capacity depends on empirical equations that are not sufficiently precise. Energy dissipation can be defined by the sum of the energy dissipated by concrete and reinforcing steel eq. (1).

$$E_D = E_{concrene} + E_{steel} \qquad ..... (1)$$

Where E_D = the dissipated energy during cyclic loading, $E_{concrene}$, E_{steel} = the energy dissipated by concrete and reinforcing steel, respectively.

Concrete is a brittle material composed of aggregates and matrix. Therefore, if cyclic loading is repeated at a specific displacement, concrete dissipates considerably less energy than reinforcing steel exhibiting plastic behavior does, For the reason, the overall dissipated energy of the member is equivalent to the sum of the energy dissipated by flexural rebars arranged in the member.

$$E_D \equiv E_{steel} \qquad ..... (2)$$

Energy dissipation capacity relies on various parameters such as reinforcement ratio, an arrangement of reinforcing bars, and the shape and size of the members' cross-sections. Thus, such empirical methods cannot accurately estimate the energy dissipation capacity, and as a result, they

decrease the overall accuracy of the evaluation method [11, 12]. The energy input to the structure subjected to earthquake ground motion is dissipated in part by inelastic deformation (hysteretic energy) and in part by viscous damping. Only hysteretic energy is assumed to participate in structural damage. The hysteretic to input energy ratio is an important response parameter that shows the range of damage in the structure. Fajfar, et al. [13] introduced a dimensionless parameterγ, which represents the relationship between hysteretic energy and the maximum displacement. This is an important energy-based damage indicator.

$$\gamma = \frac{\sqrt{E_H/m}}{\omega D} \qquad \text{….. (3)}$$

where E_H is the dissipated hysteretic energy, D is the maximum displacement, m is the mass of the system and ω is natural frequency. The parameter γ also controls the decrease of displacement ductility due to low cycle fatigue.

2.4.2 Review of Energy-based damage parameters

Manfredi [14] noted that the definition of damage is possible, based on the assumption that the structural collapse occurs when the hysteretic energy dissipated under seismic actions is equal to the energy disputed under monotonic load. The estimation of the input energy appears a first towards the definition of damage potential capable of taking into account the effect of the duration of the ground motions.

Park and Eom [15] found that the concrete which is a brittle material does not dissipate energy significantly through repeated cyclic loading. So, the energy dissipation of the reinforced concrete member is almost similar to the energy dissipated by flexural re-bars arranged in the member. It can be determined by the number of re-bars and the differential stains that the re-bars practice during cyclic loading.

Negulescu and Wijesundara [16] found that no important effects of the number of inelastic cycles to the damage estimation results for low ductile structures. It focuses on the importance of accounting for the effects of the number of inelastic cycles to the damage assessment for the high ductile structures.

3. Codal Provisions

It is widely recognized that ground shaking in existing buildings located in seismic regions may induce unacceptable levels of damage. Several reasons have been attributed to this vulnerability, such as insufficient strength and stiffness, weak detailing, plan and elevation irregularities, the dominance of brittle failure modes over ductile ones, etc. [17]. Various codes display the principle concepts for finding the performance level.

3.1. ATC-40[18]

Capacity Spectrum Method (CSM) has gained considerable popularity amongst pushover users and the ATC40 guidelines [18] included it as the recommended nonlinear static procedure to be used**.** The CSM was created to describe a structure's first mode response based on the assumption that the main response of the structure is the fundamental mode of vibration. The results obtained with the CSM may not be so accurate. The steps of the capacity spectrum method are described herein.

Step (1): Seismic Data
A MDOF model of the building must be developed including the nonlinear force-deformation relationship for structural elements under monotonic loadings, Fig. 1a. An elastic acceleration response spectrum is also required corresponding to the seismic action under consideration, Fig. 1b.
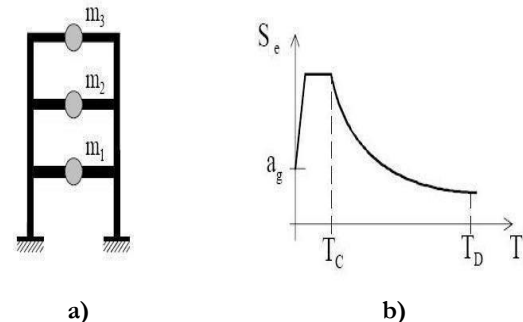

| a) | b) |

Figure (1): a) MDOF model of the building; b) Elastic acceleration response spectrum [19].

Step (2): Seismic demand in AD (acceleration displacement) format.
The seismic demand is defined with a response spectrum in the format acceleration- displacement (ADRS). For SDOF, the displacement spectrum can be computed from the acceleration spectrum using eq. (4):

$$S_d = \frac{T^2}{4\pi^2} S_e \qquad \text{…. (4)}$$

Where S_a and S_d are the values for the elastic acceleration and displacement spectrum, respectively.

Step (3): Pushover Analysis
A conventional non-adaptive force-based pushover analysis is performed, applying to the structure a monotonically increasing pattern of lateral forces. In CSM the lateral forces applied have a first mode proportional distribution. Lateral forces are applied in proportion to the storey masses and the square height of the floor as per by using eq. (5):

$$F_i = \frac{m_i h_i^2}{\sum_{j=1}^n m_j h_j^2} \qquad \text{……. (5)}$$

where, m_i and hi are the mass and height of ith floor.
From the pushover analysis one obtains the capacity curve that represents the base shear and the displacement at the center of mass of the roof.

Step (4): Equivalent SDOF system
The structural capacity curve expressed in terms of roof displacement and base shear is then converted into a SDOF curve in terms of displacements and accelerations, which is called the capacity spectrum. The transformations are made using the following equations:

$$PF_1 = \left[\frac{\sum_{i=1}^{N}(w,\phi_{i1})/g}{\sum_{i=1}^{N}(w_i\phi_{i1}^2)/g}\right] \quad \dots (6)$$

$$\alpha_1 = \frac{\left[\sum_{i=1}^{N}(w_i\phi_{i1})/g\right]^2}{\left[\sum_{i=1}^{N}w_i/g\right]\left[\sum_{i=1}^{N}(w_i\phi_{i1}^2)/g\right]} \quad \dots (7)$$

$$S_a = \frac{V/W}{\alpha_1} \quad \dots (8)$$

$$S_d = \frac{\Delta_{roof}}{PF_1\phi_{roof.1}} \quad \dots (9)$$

Fig. Fig. 2. It shows that the participation factor and modal mass coefficient differ according to the relative inter-storey displacement over the height of the building. For example, for a linear distribution of inter-storey displacement along the height of the building $\alpha_1 \approx 0.8$ and $PF_1 \approx 1.4$.
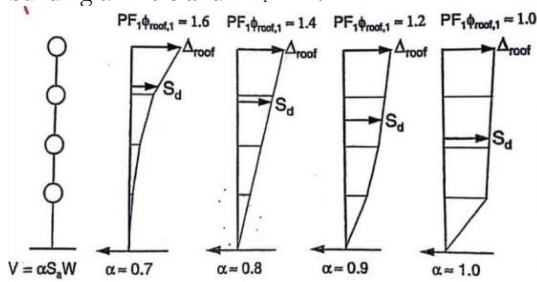

Figure (2): Modal participation factors and modal mass coefficients [18].

To convert MDOF capacity curve to SDOF capacity curve in the format (capacity spectrum) of the Acceleration-Displacement Response Spectra (ADRS) format (S_a versus S_d), the modal participation factor PF_1 and the modal mass coefficient α must first be calculated by eq. (7) and eq.(8) Afterwards, for each point of the MDOF capacity curve (V, Δroof) calculate the associated point (S_a, S_d) of the capacity spectrum according to eq.(8) and eq.(9).

Step (5): Estimation of Damping and Reduction of the Response Spectrum:

ATC-40 defines an equivalent viscous damping to represent this combination; it can be calculated using eq. (10):

$$\beta_{eq} = \beta_1 + 5 \quad \dots (10)$$

ATC-40 introduces the concept of effective viscous damping that can be obtained by multiplying the equivalent damping by a modification factor k by using eq.(11):

$$\beta_{eff} = k\beta_1 + 5 \quad \dots (11)$$

where 5 – 5% viscous damping inherent in the structure (given to be constant).

The hysteretic damping represented as equivalent viscous damping can be calculated by using eq. (12):
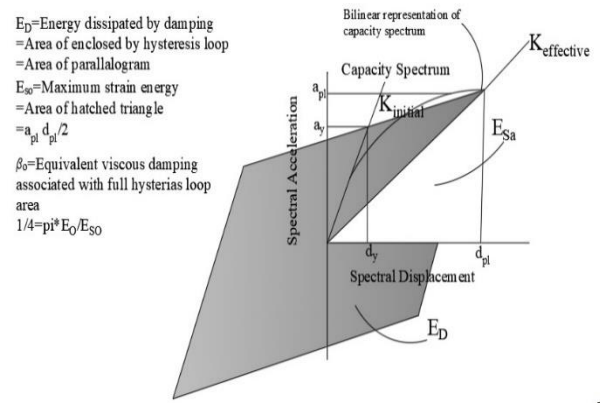
$$\beta_1 = \frac{1}{4\pi} \cdot \frac{E_D}{E_{S_0}} \quad \dots (12)$$

Figure (3): Derivation of Damping for Spectral Reduction

The physical meaning of both E_D and E_{S0} is represented in Fig.3. E_D is the energy dissipated by the structure in a single cycle of motion, that is, the area bounded by a single hysteresis loop. E_{S0} is the maximum strain energy related to that cycle of motion that is, the area of the hatched triangle. Fig. 4. Show the derivation of energy dissipated by damping.
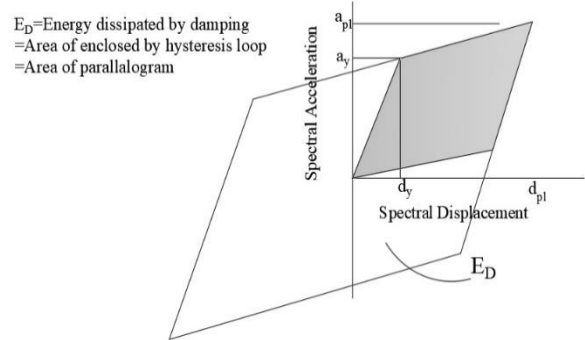

Figure (4): Derivation of energy dissipated by damping, ED.

Therefore, β_1 can be written as:

$$\beta_1 = \frac{63.7(a_y d_{pi} - d_y a_N)}{a_{pi}d_{pi}} \quad \dots (13)$$

The effective damping can be written as:

$$\beta_{eff} = \frac{63.7k(a_y d_{pi} - d_y a_{pi})}{a_{pi}d_{pi}} + 5 \quad \dots (14)$$

The *k*-factor depends on the structural behavior of the building, which is related to the seismic resisting system quality and the ground shaking duration. ATC40 defines three categories of structural behavior:

Type A represents stable, reasonably full hysteresis loops.

Type B represents a moderate reduction of area.

Type C represents poor hysteretic behavior with a significant reduction of loop area (severely pinched).

Table 1. indicates the ranges and limits for the values of *k* specified to the three structural behavior types.

Table (1): Modification factor k.

Structural Behavior Type	β_1	k
Type A	≤ 16.25	1.0
	>16.25	$1.13 - \dfrac{0.51(a_y d_{pi} - d_y a_{pi})}{a_{pi} d_{pi}}$
Type B	≤ 2.5	0.67
	>2.5	$0.845 - \dfrac{0.446(a_y d_{pi} - d_y a_{pi})}{a_{pi} d_{pi}}$
Type C	Any value	0.33

Step (6): Numerical Derivation of Spectral Reduction

The spectral reduction factors are calculated as shown in eq. (15) and eq. (16).

$$SR_A = \frac{3.21 - 0.68 \ln(\beta eff)}{2.12} =$$
$$\frac{3.21 - 0.68 \ln\left[\frac{63.7 k (a_y d_{pi} - d_y a_{pi})}{a_m d_{pi}} + 5\right]}{2.12} \geq \text{Value in Table(2)}$$
$$\ldots\ldots (15).$$

$$SR_v = \frac{2.31 - 0.41 \ln(\beta eff)}{1.65} =$$
$$\frac{2.31 - 0.41 \ln\left[\frac{63.7 k (a_y d_{ri} - d_y a_{pi})}{a_{pi} d_{pi}} + 5\right]}{1.65} \geq \text{Value in Table(2)}$$
$$\ldots\ldots (16).$$

Note that the SR_A and SR_v values should be greater than or equal to the values referred to in Table 2.

Table (2): The minimum allowable SR_A and SR_v values

Structural Behavior Type	SR_A	SR_v
Type A	0.33	0.50
Type B	0.44	0.56
Type C	0.56	0.67

Step (7): Calculation of the target displacement:

The calculation of the target displacement is an iterative process, where it is necessary to estimate a first trial performance point. For this purpose, there are several options one can use:

1. The first trial performance point can be estimated as the elastic response spectrum displacement corresponding to the elastic fundamental period. The response spectrum is defined for the viscous damping level considered (in buildings one usually considers 5%);

2. Consider a first trial equivalent damping value, for example 20%, and calculate the respective reduction factor. Multiply the elastic spectrum by this reduction factor and intersect the capacity curve with the reduced spectrum. The intersection corresponds to the first trial performance point.

The capacity curve is then bilinearized for this point, and a new effective damping can be computed and

hence a new reduction factor can be applied. The new intersection between the capacity curve and the new reduced spectrum leads to a new performance point. If the target displacement calculated is within a tolerable range (for example within 5% of the displacement of the trial performance point), then the performance point can be obtained. Fig.5. represents the process schematically.
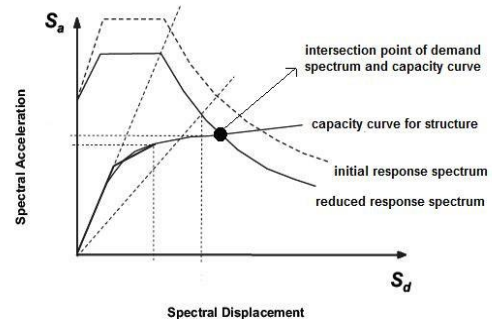

Figure (5): General CSM procedure to compute the target displacement.

Step (8): Determination of MDOF response parameters in correspondence to the Performance Point (converted from SDOF to MDOF)

At this stage of the procedure, one should go back to the MDOF pushover curve to the point consistent to the value of the SDOF target displacement (calculated in the previous step) multiplied by the transformation factor. For this step, one should take the building's performance results, such as deformations, inter storey drifts and chord rotations.

3.2. FEMA273/356 [20,21]

The Displacement Coefficient Method (DCM) is the primary nonlinear static procedure presented in FEMA 356. The target displacement, δ, at each floor level shall be calculated in accordance with eq. (17):

$$\delta_t = C_0 C_l C_2 C_3 S_a \frac{T_e^2}{4\pi^2} g \qquad \ldots\ldots (17)$$

where:

C_0 = Modification factor to associate spectral displacement of an equivalent SDOF system to the roof displacement of the building MDOF system determined using one of the following procedures:

1. The first modal participation factor at the level of the control node.
2. The appropriate value from Table 3.

Table (3): Values for Modification Factor C_0

No. of stories	Modification Factor
1	1.0
2	1.2
3	1.3
5	1.4
+10	1.5

C_1 = Modification factor to associate with estimated maximum inelastic displacements to displacements calculated for linear elastic response:

= 1.0 for $T_e \geq T_S$

= $[1.0 + (R-1)T_s/T_e]/R$ for $T_e < T_S$

C_1 not greater than the values below, and no less than 1.0.

$$C_1 = \begin{cases} 1.5 \text{ for } T_e < 0.1\text{s} \\ 1.0 \text{ for } T_e \geq T_s \end{cases}$$

T_e = Effective fundamental period of the building in the direction under consideration.

$$T_e = T_i \sqrt{\frac{K_i}{K_e}} \qquad \text{……. (18)}$$

R= Ratio of elastic strength demand to calculated yield strength coefficient.

$$R = \frac{S_a}{V_y/W} \cdot C_m \qquad \text{…. (19)}$$

C_2 = Modification factor to represent the influence of pinched hysteretic shape, stiffness and strength degradation on maximum displacement response. Values of for different framing systems and Structural Performance Levels shall be calculated from Table 4.

Table (4): Values for Modification Factor C2

Structural performance level	T≤ 0.1 second		T ≥Tₛ second	
	Framing type 1[1]	Framing type 2[2]	Framing type 1[1]	Framing type 1[2]
Immediate Occupancy	1.0	1.0	1.0	1.0
Life Safety	1.3	1.0	1.1	1.0
Collapse Prevention	1.5	1.0	1.2	1.0
[1.]Structures in which more than 30% of the floor shear at any level is resisted by any combination of the following elements, elements, or frames: ordinary moment-resisting frames, concentrically-braced frames, frames with partially-restrained connections, tension-only braces, unreinforced masonry walls, shear-critical, piers, and spandrels of reinforced concrete or masonry.				
[2.] All frames not assigned to Framing Type 1.				

C_3= Modification factor due to dynamic P-Δ effects to represent increased displacements. For buildings with a positive post-yield stiffness (maintains its strength during a given deformation cycle, but loses strength in subsequent cycles, the effective stiffness also decreases in subsequent cycles (degradation of cyclic strength)) the value shall be set at 1.0.For buildings with negative post-yield stiffness(Note that the degradation happens during the similar cycle of deformation in which yielding occurs, resulting in a negative post-elastic stiffness, (in-cycle strength degradation)), values of shall be calculated using eq.(20)

$$C_3 = 1.0 + \frac{|\alpha|(R-1)^{3/2}}{T_e} \qquad \text{…. (20)}$$

Where α is the ratio of post yield stiffness to elastic stiffness when the nonlinear force-displacement relation is characterized by a bilinear relation.

3.3. FEMA440 [22]
▪ **Improved Procedures for Displacement Modification**

FEMA 440 (2005) [22] advises that the restrictions (capping) of the C1 coefficient permitted by FEMA 356 be abandoned. A distinction between

two different types of strength deterioration that have different effects on system response and performance is also recognized. This distinction gives rise to recommendations for the C2 coefficient to account for cyclic strength and stiffness degradation. It is also recommended that the coefficient C3 be removed and replaced with a limitation on strength (R).

a. Maximum Displacement Ratio (Coefficient C₁)

FEMA 356 currently accepts the coefficient C_1 to be restricted (capped) for relatively short-period structures. FEMA440 suggested that this limitation not be used. This may increase estimates of displacement for some structures. For most structures the following simplified expression may be used for the coefficient C_1:

$$C_1 = 1 + \frac{R-1}{aT_e^2} \qquad \text{…. (21)}$$

For periods less than 0.2 s, the value of the coefficient C_1 for 0.2 s may be used. For periods greater than 1.0 s, C_1 may be assumed to be 1.0.

b. Degrading System Response (CoefficientC₂)

FEMA 356 suggested that the C_2 coefficient represent the influences of stiffness degradation only. FEMA440 recommended that the displacement prediction be modified to account for cyclic degradation of stiffness and strength. It recommended that the C_2 coefficient be as follows:

$$C_2 = 1 + \frac{1}{800}\left(\frac{R-1}{T}\right)^2 \qquad \text{……. (22)}$$

For periods less than 0.2 s, the value of the coefficient C_2 for 0.2 s may be used. For periods greater than 0.7 sec. C_2 may be assumed equal to 1.0 for assumption would include buildings with modern concrete or steel special moment-resisting frames, steel eccentrically braced frames, and buckling-restrained braced frames as either the original system or the system added during seismic retrofit.

c. P-Δ Effects (Coefficient C₃)

Because of dynamic P-Δ effects, the displacement modification factor C3 is intended to account for increased displacements. FEMA 440 proposed removing the current coefficient of C3 and replacing it with the maximum strength ratio, R, intended to calculate dynamic instability. Where the value for R_max is exceeded, a Nonlinear Dynamic Procedures (NDP) analysis is recommended to capture strength degradation and dynamic P-Δ effects to confirm dynamic stability of the building. Nonlinear static procedures are not capable of distinguishing completely between cyclic and in-cycle strength losses. However, insight can be obtained by separating the in-cycle P-Δ effects from α₂, Fig.6.
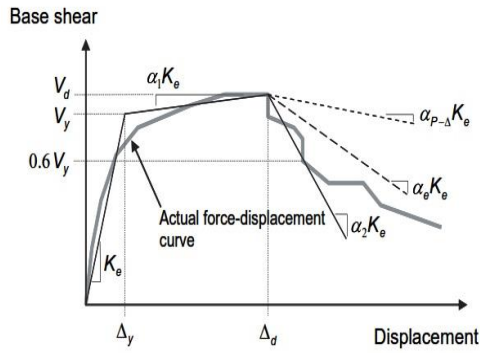
Figure (6): Idealized Force-Displacement Curves.

An effective post-elastic stiffness can then be determined as

$$\alpha_e = \alpha_{p-\Delta} + \lambda(\alpha_2 - \alpha_{p-\Delta}) \quad \dots (23)$$

Where $0 \leq \lambda \leq 1.0$

FEMA 440 recommended that λ be assigned a value of 0.2 for sites not subject to near field effects and 0.8 for those that are. Displacement amplifications increase as the post-yield negative stiffness (caused by in-cycle strength degradation) ratio α decreases (becomes more negative), as R increases. Minimum strength (maximum R) required avoiding dynamic instability. The recommended limitation on the design force reduction, R_{max}, is as follows

$$R_{max} = \frac{\Delta_d}{\Delta_y} + \frac{|\alpha_e|^{-t}}{4} \quad \dots (24)$$

Where

$$t = 1 + 0.15 \ln T \quad \dots (25)$$

The structural model must appropriately model the strength degradation characteristics of the structure and its components.

▪ **Improved Procedures for Equivalent Linearization**

An improved equivalent linearization procedure as adjustment to the Capacity-Spectrum Method (CSM) of ATC-40[18]. When equivalent linearization is used as a part of a nonlinear static procedure that models the nonlinear response of a building with a SDOF oscillator, the objective is to evaluate the maximum displacement response of the nonlinear system with an "equivalent" linear system using an effective period, T_{eff}, and effective damping, β_{eff}, Fig.7.
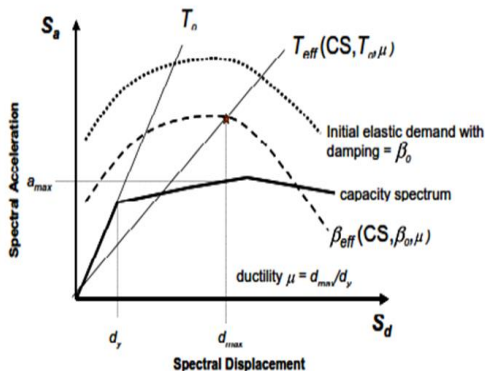

Figure (7): Effective period and damping parameters of the equivalent linear system

a. Effective damping

The formulas herein presented apply to any capacity curve, independent of hysteretic model type or post-elastic stiffness value (α) used. The effective damping is calculated using Equations below depending on the structure's level of ductility μ.

For $\mu < 4.0$:

$$\beta_{eff} = 4.9(\mu - 1)^2 - 1.1(\mu - 1)^3 + \beta_0 \dots (26)$$

For $4.0 \leq \mu \leq 6.5$:

$$\beta_{eff} = 14.0 + 0.32(\mu - 1) + \beta_0 \quad \dots (27)$$

For $\mu > 6.5$:

$$\beta_{eff} = 19\left[\frac{0.64(\mu-1)-1}{[0.64(\mu-1)]^2}\right]\left(\frac{T_{eff}}{T_0}\right)^2 + \beta_0 \quad \dots (28)$$

b. Effective period

The following equations apply to any capacity spectrum independent of hysteretic model form or post-elastic stiffness value. The effective period depends on the ductility level and is calculated using Equations below:

For $\mu < 4.0$:

$$T_{eff} = \{0.20(\mu - 1)^2 - 0.038(\mu - 1)^3 + 1\}T_0 \quad \dots (29)$$

For $4.0 \leq \mu \leq 6.5$:

$$T_{eff} = [0.28 + 0.13(\mu - 1) + 1]T_0 \quad . (30)$$

For $\mu > 6.5$:

$$T_{eff} = \left\{0.89\left[\sqrt{\frac{(\mu-1)}{1+0.05(\mu-2)}} - 1\right] + 1\right\}T_0 \quad \dots (31)$$

Where α is the post-elastic stiffness and μ the ductility, calculated as follows

$$\alpha = \frac{\left(\frac{a_{pi}-a_y}{d_{pi}-d_y}\right)}{\left(\frac{a_y}{d_y}\right)} \quad \dots (32)$$

and

$$\mu = \frac{d_{pi}}{d_y} \quad \dots (33)$$

c. Spectral reduction factor for effective damping

The spectral reduction factor is a function of the effective damping and is called the damping coefficient, B(βeff) and is calculated using Equation

$$B(\beta_{eff}) = \frac{4}{5.6 - \ln \beta_{eff}(in\%)} \quad \dots (34)$$

It is used to adjust spectral acceleration ordinates as shown in eq.35.

$$(S_a)_\beta = \frac{(S_a)_{5\%}}{B(\beta_{eff})} \quad \dots (35)$$

3.4. ASCE 41-06 [23]

ASCE41-06 depends on the displacement coefficient method to capture the target displacement. The target displacement, δ at each floor level shall be determined in accordance with eq.36.

$$\delta_t = C_o C_1 C_2 S_a \frac{T_e^2}{4\pi^2} g \quad \dots (36)$$

where C_o = modification factor to relate spectral displacement of an equivalent single-degree of freedom (SDOF) system to the roof displacement of the building. Multi-Degree Of Freedom (MDOF) system determined using one of the following procedures:

1. The first mode mass participation factor multiplied by me ordinate of the first mode shape at the control node.
2. The mass participation factor calculated Using a shape vector corresponding to the deflected shape of the building at the target displacement multiplied by ordinate of the shape vector at the control node.
3. The appropriate value from Table.5.

Table (5): Values for Modification Factor Co

| No. of stories | Shear Buildings[1] | | Other Buildings |
	Triangular load pattern	Uniform load pattern	Any load pattern
1	1.0	1.0	1.0
2	1.2	1.15	1.2
3	1.2	1.2	1.3
5	1.3	1.2	1.4
+10	1.3	1.2	1.5
[1]Buildings in which, for all stories, story drift decreases with increasing height.			

C_1 = factor of modification to relate the estimated maximum inelastic displacements to the linear elastic response displacements calculated. For periods less than 0.2 sec, C, need not be taken greater than the value at T = 0.2 sec. For periods greater than 1.0 sec, C_1 = 1.0.

$$C_1 = 1 + \frac{R-1}{aT_e^2} \quad \text{.... (37)}$$

where
a = site class factor:
= 130 site Class A, B;
= 90 site Class C;
= 60 site Class D, E, F;
C_2 = modification factor to represent the influence of pinched hysteresis shape, cyclic stiffness degradation, and strength deterioration on maximum displacement response. For periods greater than 0.7 sec, C_2 =1.0;

$$C_2 = 1 + \frac{1}{800}\left(\frac{R-1}{T_e}\right)^2 \quad \text{....... (38)}$$

- The strength ratio R shall be calculated in accordance with eq.39.

$$R = \frac{S_a}{V_y/W} \cdot C_m \quad \text{....... (39)}$$

- C_m taken as the effective modal mass participation factor determined for the fundamental mode using an Eigenvalue analysis shall be acceptable. C_m shall be taken as 1.0 if the fundamental period, T, is greater than 1.0 sec.

For buildings with negative post-yield stiffness, the maximum strength ratio, R_{max} shall be calculated in accordance with eq.41.

$$R_{war} = \frac{\Delta_d}{\Delta_y} + \frac{|\alpha_d|^{-h}}{4} \quad \text{.... (40)}$$

where
Δ_d = lesser of target displacement, or displacement at maximum base shear defined in Figure (7)
Δ_y = displacement at effective yield strength defined in Fig. (7).
h = 1 + 0.15. In T, and

α_e= effective negative post-yield slope ratio defined in eq.41.

$$\alpha_e = \alpha_{p-\Delta} + \lambda(\alpha_2 - \alpha_{p-\Delta}) \quad \text{.... (41)}$$

where
α_2 = negative post-yield slope ratio defined in Figure (6). This contains P-A effects, in-cycle degradation, and cyclic degradation;
α p-Δ = negative slope ratio caused by P-Δ effects; and
λ = near field effect factor:
= 0.8 if $S_1 \leq 0.6$ (Maximum Considered Earthquake, MCE); = 0.2 if $S_1 < 0.6$ (MCE).

3.5. Euro code 8 [24]

N2 method, first proposed by Fajfar and Fischinger [24] and subsequently developed by Fajfar[25][26, 27], is the Nonlinear Static Procedures (NSP) adopted by Euro code 8[23] and is a modified version of the CSM. Indeed, the estimation of seismic demand is based on the use of inelastic spectra in the N2 method instead of highly damped elastic spectra, as per the CSM. The steps of the capacity spectrum method are defined herein.

Step (1) and **Step (2)** are the same steps of capacity spectrum method with ATC-40[18].

Step (3): Pushover analysis
A pushover analysis is performed, applying to the structure a monotonically increasing pattern of lateral forces, Fig.8. These forces represent the inertial forces induced in the structure by the ground motion. Any reasonable distribution of lateral loads can be used in the N2 method. The Euro code 8 recommends the use of at least two distributions: a first mode proportional load pattern and a uniform load pattern.

The vector of the lateral loads $\bar{F}$ used in the pushover analysis proportional to the first mode is determined as:

$$\bar{F} = pM\Phi \quad \text{.... (42)}$$

The lateral force in the i-th level is proportional to the component Φ of the assumed displacement shape Φ_i, weighted by the story mass m_i

$$\bar{F} = pm_i\Phi_i \quad \text{.... (43)}$$

The vector of the lateral loads $\bar{F}$ used in the pushover analysis with a uniform distribution is determined as:

$$\bar{F}_{uni} = pM \quad \text{.... (44)}$$
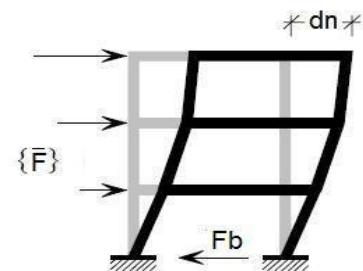$$\bar{F}_{unij} = pm_i \quad \text{.... (45)}$$

Figure (8): Pushover analysis of the MDOF model
The **N2** method prescribes that this curve should represent the base shear (F_b) and the displacement at the center of mass of the roof (d_n).

Step (4): Equivalent SDOF system

The MDOF structure should be transformed into an equivalent SDOF system. The definition of the transformation factor Γ is based on the equation of motion of a MDOF system.

$$M \cdot \ddot{U} + R = -M \cdot 1 \cdot a \quad .... (46)$$

Where, U is the displacement vector, $\ddot{U}$ is the acceleration vector, M is a diagonal mass matrix, R is the internal forces vector, 1 is a unit vector and a is the ground acceleration as a function of time. The deformed pattern Φ is assumed to be constant during the structural response to the earthquake. The displacement vector is then written as eq.47.

$$U = \Phi \cdot d_n \quad .... (47)$$

where d_n the time dependent top displacement. The Φ is normalized in order to have its component at the top equal to 1. The internal forces R are equal to the statically applied external loads $\bar{F}$.

$$\bar{F} = R \quad .... (48)$$

Equations (42 and 47) into Equation (46) and multiplying the equation by Φ, it follows:

$$\Phi^T \cdot M \cdot \Phi \cdot \dot{d}_n + \Phi^T \cdot M \cdot \Phi \cdot p = -\Phi^T \cdot M \cdot 1 \cdot a ... (49)$$

The equation of motion of the SDOF system can be written as:

$$m^* \cdot \ddot{d}^* + F^* = -m^* \cdot a \quad .... (50)$$

where m^* is the equivalent mass of the SDOF system and it is calculated using eq.51.:

$$m^* = \Phi^T \cdot M \cdot 1 = \Sigma m_i \Phi_i \quad .... (51)$$

The transformation of the MDOF to the SDOF system is made in the N2 method using eq.52 and eq.53.

$$d^* = \frac{d_n}{\Gamma} \quad .... (52)$$

$$F^* = \frac{F_b}{\Gamma} \quad .... (53)$$

where d^*, F^* are the displacement and base shear of the SDOF system. The transformation factor Γ from the MDOF to the SDOF model is defined according eq.54:

$$\Gamma = \frac{\Phi^T \cdot M \cdot 1}{\Phi^T \cdot M \cdot \Phi} = \frac{\Sigma m_i \Phi_i}{\Sigma m_i \Phi_i^2} = \frac{m^*}{\Sigma m_i \Phi_i^2} = \frac{\Sigma F_i}{\Sigma\left(\frac{F_i^2}{m_i}\right)} ... (54)$$

The transformation factor Γ is usually called the modal participation factor. The SDOF capacity curve is defined by the displacement of the SDOF (d^*) and base shear of this system (F^*) as shown in Fig.9.
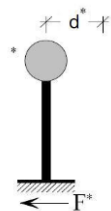

Figure (9): Equivalent SDOF system.

Euro code 8 prescribes a simplified elastic-perfectly plastic bilinear approximation of the SDOF capacity curve.
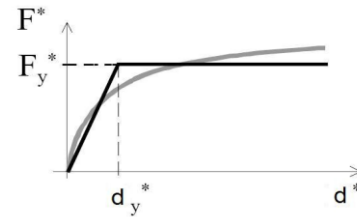

Figure (10): SDOF capacity curve and its bi linearization

The elastic period of the idealized bilinear SDOF system T* is computed according to eq.55:

$$T^* = 2\pi \sqrt{\frac{m^* d_y^*}{F_y^*}} \quad .... (55)$$

N2 method assumes that in the medium/long period range (T*≥T$_c$) the equal displacement rule applies, i.e. the displacement of the inelastic system S$_d$ is equal to the displacement of the associated elastic system S$_{de}$ characterized by the same period T*, where T$_c$ is the characteristic period of the ground motion, which is defined as the transition period between the constant acceleration section of the response spectrum (corresponding to the short period range) and the constant velocity segment of the response spectrum (corresponding to the medium period range) Fig.11.
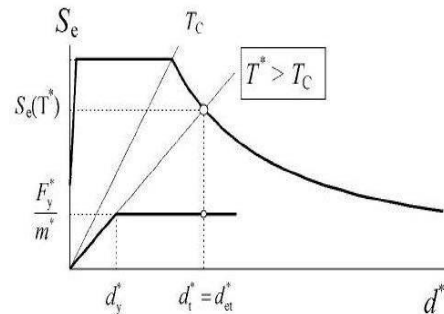

Figure (11): Long period range.

This means Rμ= μ in the above-mentioned period range. Seismic demand in terms of inelastic displacement can be obtained by intersecting the radial line with the elastic demand spectrum corresponding to the SDOF system period. In the case of short-period structures (T*< T$_C$) the inelastic displacement is larger than the elastic one and the equal displacement rule does not apply anymore Fig.12. Consequently R_μ< μ and it can be calculated as the ratio between the elastic acceleration demand capacity S$_{ae}$ and the inelastic acceleration S$_{ay}$. The inelastic displacement demand is, in this case, equal to S$_d$= μ ·D$^*_y$ being D$^*_y$ the yielding displacement of the SDOF system. The ductility factor can be derived from the reduction factor by the relation:
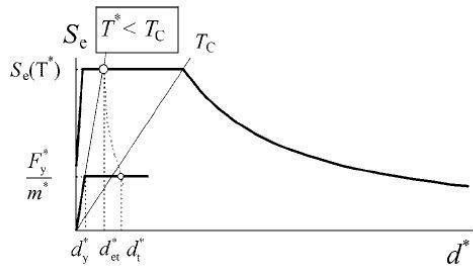
$$\mu = (R_\mu - 1)\frac{T_C}{T^*} + 1 \quad .... (56)$$

Figure (12): Short period range.

In both cases (T*≥Tc and T*<TC) the inelastic acceleration demand S_a is equal to the elastic one S_{ae} and it can be verified at the intersection of the radial line corresponding to the period of the SDOF system with the elastic demand spectrum.

3.6 Japanese Standard [25]

Three screening levels have been introduced in the Japanese standard (2001) for seismic capacity evaluation. Seismic index of the structure for each story

$$I_s = E_o.S_D.T \qquad ……(57)$$

where E_o is the primary seismic index of screening levels. The primary seismic index of structure E_o of the i-th story in an n-story building is given as a product of strength index. **C**, ductility index **F** and α is the effective strength factor, differently in each screening levels as shown in table below.

S_D is introduced to adjust the basic seismic index by measuring the effects of horizontal and vertical shapes, and the mass and stiffness irregular distribution of the structure.

T is a modification factor of the basic seismic index which evaluates the effects of cracks, deflection, and aging of building. T value will be at range 0.7 to 0.9 but if there is no defect, the T value is 1. Building older than 30 years have a T value of 0.8, but for newer buildings less than 19 years old the T value should be equals to 1.

Table (6): Values of primary seismic index (E_o)

Screening	primary seismic index (E_o)
First Screening	$E_0 = \dfrac{n+1}{n+i}(C_w + \alpha_1 C_e) \times F_w$
Second Screening	$E_0 = \dfrac{n+1}{n+i}(C_{sc} + \alpha_2 C_w + \alpha_3 C_c) \times F_{sc}$
Third Screening	$E_0 = \dfrac{n+1}{n+i}\sqrt{E_1^2 + E_2^2 + E_3^2}$
Forth Screening	$E_0 = \dfrac{n+1}{n+i}\left(C + \sum_j \alpha_j C_j\right) \times F_1$

Seismic demand index(I_{so}) regardless of the number of stories in the building:

$$I_{so} = Es.Z.G.U \qquad ……(58)$$

where

Es is the basic seismic demand index of the structure, standard values of which shall be selected as 0.8 for the first level screening and 0.6 for the second and third level screenings.

Z is zone index, namely the modification factor accounting for the seismic activities and intensities expected in the region of the site.

G is a ground index, namely the modification factor accounting for the effects of the amplification of the surface soil, geological conditions and soil-and-structure interaction on the expected earthquake motions.

U is the usage index, namely the modification factor accounting for the building.
If

$$Is \geq Iso \qquad … (59)$$

If eq.59 is satisfied, the building may be assessed to be "safe". Otherwise, the building should be assessed to be "an uncertainty" in seismic safety and need to retrofit.

3.7 ZS1170.5 2004[26]

The target displacement of NZS1170.5 2004is calculated by using the coefficient method as described in FEMA-356.

$$\delta = C_0 C_1 C_2 C_3 C(T)\frac{T_c^2}{4\pi^2}g \qquad …….(60)$$

where the coefficients take the same roles in modifying the expected elastic displacement Expressions for them are redefined here to better reflect the intent of NZS1170.5.

C_0 will equal "1" as we plot the deflection of the dynamic center of mass.

C_1 accounts for the variation between the response of an elasto-plastic and elastic SDF systems and can be obtained from clauses 5.2 and 7.2.1.1 of the Standard expressed as

$$C_1 = \mu^* Sp/k_\mu \qquad …….(61)$$

C_2 will equal "1" as there is no account made in NZS1170.5 for differences in response of systems with a pinched hysteretic shape and stiffness and strength degradation.

C_3 is to account for the increased displacements resulting from dynamic P-delta effects. This can be derived from the Standard as

$$C_3 = 1 + \beta\theta \qquad ………(62)$$

NZS1170.5 provides limitations as to which buildings require P-delta effects included in the analyses. This is a pragmatic approach to allow simple regular buildings to be quickly designed with the knowledge that other conservative clauses in the Standard will provide for the shortfall in strength. It is recommended here, that where the NSP procedure is used in aseismic assessment procedure and the building has not been designed to modern Standards, C_3 as per Eq.8 be included in the analysis of all buildings**(T)** is the ordinate of the elastic hazard spectrum as per clause 3.1.1 of the Standard.

3.8 IS-15988(2013) [27]

Recommendation for Detailed Evaluation:

A building is recommended to undergo a detailed evaluation, if any of the following conditions are met:
a) Building fails to comply with the requirements of the preliminary evaluation;
b) A building is 6 stories and higher;
c) Buildings located on incompetent or liquefiable soils and/or located near (less than 15 km) active faults and/or with inadequate foundation details; and

d) Buildings with inadequate connections between primary structural members, such as poorly designed and/or constructed joints of pre-cast elements.

If acceptability criteria satisfied, the retrofit **not** recommended.

Detailed Evaluation (for primary lateral-force resisting system):

a) Evaluation Procedures

1. Probable Flexure and Shear Demand and Capacity

Estimate the probable flexural and shear strengths of the critical sections of the members and joints of vertical lateral force resisting elements. These calculations shall be performed as per respective codes for various building types and modified with knowledge factor K.

2. Design Base Shear

Calculate the total lateral force (design base shear) in accordance with [IS 1893 (Part 1)] and multiply it with U, a factor for the reduced useable life (equal to 0.70).

3. Analysis Procedure

Perform a linear equivalent static or a dynamic analysis of the lateral load resisting system of the building in accordance with IS 1893 (Part 1) for the modified base shear determined in the previous step and determine resulting member actions for critical components.

a) Mathematical model: The physical structure's mathematical model is designed to represent the spatial distribution of the mass and the stiffness of the structure to the extent that it is adequate to calculate the significant characteristics of its lateral force distribution. Both elements of concrete as well as masonry must be used in the model.

b) Component stiffness: Component stiffness shall be determined based on some rational procedure

4. It must compare probable component strength with expected seismic demands.

Acceptability Criteria

A building is said to be acceptable if one of the following two requirements, along with additional criteria for a specific form of building, are met:

a) All critical elements of lateral force resisting elements have strengths greater than computed actions and drift checks are satisfied.

b) Except a few elements, all critical elements of the lateral force resisting elements have strengths greater than computed actions and drift checks are satisfied. The engineer has to ensure that the failure of these few elements shall not lead to loss of stability or initiate progressive collapse. This needs to be verified by a non-linear analysis such as pushover analysis, carried out up to the collapse load.

3.9 Review of Codes Procedures for Seismic Assessment of Existing Buildings

Mahaylov and Petrini [28] studied five codes for evaluating existing buildings (Italian Seismic Code [29], EC8 [24], FEMA356 [21], ATC40 [18] and FEMA440 [22] were analyzed by looking at the theoretical basis of the problems. It found that the dynamic P-Δ effect is not considered by the Italian seismic code and the EC8. According to FEMA440 [22], the procedures implemented in FEMA356 and ATC-40 [21] are not able to adequately capture the dynamic instability phenomenon. The non-linear static procedure in the Italian seismic code and EC8 [24] is based on the Equivalent SDOF system's elastic-perfectly plastic nature. Degradation effects of strength and stiffness are not considered. This simplification may lead to underestimation of the target displacement.

Moshref et al. [30] used two main guidance documents, the New Zealand Guideline [31] and FEMA 440 [22], on the evaluation of existing buildings currently available for concrete frame resistance. The main aim of the study was to trace the differences between the results provided by these two guidelines. Under the two guidelines, the Peak Ground Acceleration (PGA) values that cause the collapse are calculated and compared with their similar values, which are determined from a non-linear dynamic analysis. The outcome of the force-based approach suggested by the New Zealand Guideline was found to be more consistent with nonlinear dynamic analysis. Appropriate results were given by the New Zealand displacement method and FEMA440 [22], but their results are not conservative.

Alwashali and Maeda [32] investigated the damage caused by the Great East Japan earthquake in Sendai City-Japan in 2011 to many low-rise RC buildings. Using the Japanese Standard for Seismic Evaluation of Existing RC Buildings, the chosen building is assessed to have a high seismic capacity. On those buildings, pushover analysis was performed. The pushover analysis was found to predict the degree of damage well, but there were some variations in the position of the plastic hinge compared to the actual damage. Plastic hinges were expected to occur in beams and not in columns, but this wasn't the case in the actual damage.

Xiaoguang et al. [33] studied the seismic design code for buildings in Japan (Japanese standard Code) [34], India (IS 1893-2002) [35], Turkey [36], China (GB 50011-2010) [37], Korea [38], Nepal (NBC105)[39], Indonesia (SNI-02-1726-2002)[40], and Iran (Iranian code) [41], in detail. These countries' seismic fortification parameters are contrasted by evaluating the classification of the site, the seismic effective coefficient, and the seismic spectral design. The findings indicate that China and Japan have the highest horizontal seismic activity. So in China and Japan, the seismic fortification level is high. In Turkey and Korea, the seismic fortification level is low. In most Asian countries, except the seismic design code of Korea [38], the response spectrum principle was used in the seismic design of buildings.

Araujo et al. [42] conducted a comparative analysis of the European and American seismic safety assessment procedures as described in Eurocode 8-Part3 (EC8-3) [24] and ASCE41-06 [23]. In the seismic evaluation of four separate steel buildings built according to different requirements, these two principles are used. The main results in the study are no safety checks could be performed as Eurocode 8-Part3 (EC8-3) [24] requires the analyst

to evaluate the safety of each ductile element by checking its plastic rotation capacity based on the demand obtained from a linear elastic structural model.

Hakim et al. [43] evaluated the performance of buildings that were built using pushover analysis by the Saudi Building Code (SBC 301) [44]. It examines four typical RC frame structures. To produce the ultimate building capacity, pushover analysis is performed. Building performance levels are defined by ATC-40 [18], FEMA-356[21], and FEMA-440 [22]. The findings show that all three methods suggest that the safety margin against collapse is high, adequate reserves of strength, and displacements are available. It found that the design of SBC buildings usually meets the acceptance requirements for these methods.

Cavdar and Bayraktar [45] included several performance evaluation procedures. Four main guidelines/codes describe the most common evaluation procedures: ATC-40 [18], FEMA 356 [21], FEMA 440 [22], and TEC-2007[46]. The static pushover and nonlinear time history studies analyze the nonlinear seismic behavior of a collapsed reinforced concrete (RC) residential building in Turkey. It found that the current structural structure of residential buildings did not meet the ATC-40 [18], FEMA 356 [21], FEMA 440 [22], and TEC-2007[46] predicted standards of performance (LS). According to both nonlinear static pushover analysis and time history analysis under earthquake loads, the building constructed according to TEC-1975[47] presents the level of CO performance through two-direction results.

Kurniawandy and Nakazawa [48] explained the seismic assessment of existing buildings based on a Japanese standard [25] using the seismic index method. Based on the intensity and ductility parameters, the fundamental seismic index is determined. Two existing buildings were assessed. For each story, the seismic index of the structure has a different value. The minimum seismic index exists on the ground floor, and as the number of floors increases, the index increases. If the seismic index (I_s) is higher than the seismic demand index (I_{so}), the structure is evaluated for seismic safety. It was found that the correlation between the results of the measurement of the seismic index based on the Japanese standard and the drift requirements according to the ASCE41-06 [23] was consistent, it a good method to evaluate existing structures.

4. Analytical techniques of performance evaluation

To assess the seismic performance of any structure, it is important to estimate its dynamic characteristics and to predict its response to the ground motion to which it may be exposed during its service life. Dynamic characteristics, namely periods and mode shapes, are obtained through an eigenvalue analysis [49]. As it is exposed to different levels of ground motion, the nonlinear dynamic time-history analysis provides the damage states of the building. The nonlinear study of time history can be divided into

two methods; one is based on the dynamic response of a multi-degree of freedom (MDOF) system similar to a single degree of freedom system [50], the other is based on an equivalent response directly derived from the MDOF system's nonlinear dynamic response [51]. To assess the lateral load resisting capacity of a structure and the maximum damage level to the structure at the ultimate load, nonlinear static procedure (push-over) analysis may be used. It is also possible to divide the static pushover analysis into two methods; one is based on the first (fundamental mode) pushover analysis [18], the other based on the Modal Pushover Analysis (MPA) where higher mode effects are taken into account. [52].

4.1 Nonlinear Static Analysis
4.1.1 Capacity Spectrum Method (CSM)

A performance-based seismic analysis methodology, the Capacity Spectrum Method (CSM), may be used for several purposes, such as rapid assessment of a large inventory of buildings, design verification for new construction of individual buildings, assessment of an existing structure to identify damage states, and correlation of damage states of buildings to different ground motion amplitudes. The method compares the structure's capacity (in the form of a pushover curve) with the structure's demands (in the form of a response spectrum). The graphic intersection of the two curves approximates the structure's response. Effective viscous damping values are applied to linear-elastic response spectra similar to inelastic response spectra to account for the non-linear inelastic behavior of the structural system [53]. This approach is often referred to as a pushover analysis. Fig.13.Shows the principle of the capacity spectrum method.
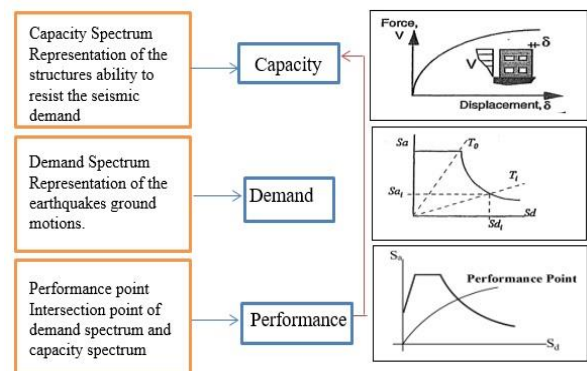

Figure (13): Demand& Capacity Curves [53].

4.1.2 Displacement Coefficient Method (DCM)

The nonlinear static procedure is introduced through the Displacement Coefficient Method. This approach modifies the SDOF system's linear elastic response by multiplying it by many coefficients from C_0 to C_3. To achieve this equivalence, these four coefficients are required to take account of the structure's inelastic behavior as well as the increase in the number of degrees of freedom. The first one (C_0) is related to the spectral displacement equivalence between both systems, the second one (C_1) takes into account the inelastic deformation, the

third one (C_2) corresponds to the effect of pinched hysteretic shape and the fourth one (C_3) is due to the dynamic (P-Δ) effects [54]. Fig.14.Show the Process Schematic of the Displacement Coefficient Method.
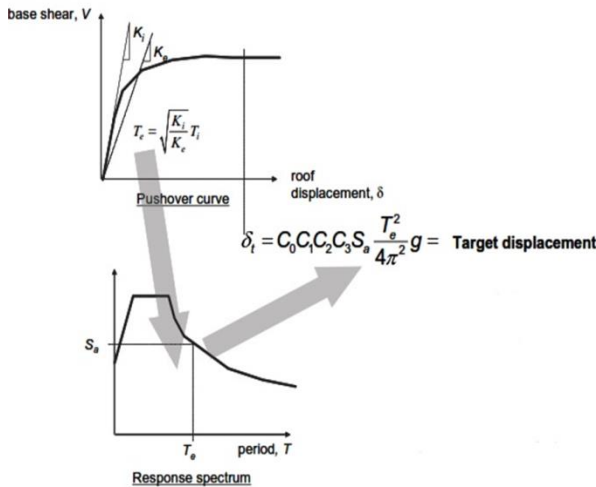

Figure (14): Process Schematic of the Displacement Coefficient Method [22].

4.2 Review of Pushover Analysis

4.2.1 Review of Pushover Analysis of an Existing Hospital Buildings

Singh et al. [55] studied the eight story ward building of GTB hospital located at Delhi-India. The brick masonry infills were modeled as strut components, the slabs were assumed as a rigid diaphragm, the plastic hinge rotation values corresponding to different performance levels were taken according to FEMA 356[21], taking into account the relations between axial force moment and shear force moment. Using both the Capacity Spectrum Method (CSM) and the Displacement Coefficient Method (DCM), with the value of coefficients as per FEMA 440[20], the performance point of the building was calculated. The result showed that the plastic deformations in beams and columns were found to be within the level of IO performance while those in masonry infills exceeded the level of CP performance. The beams and columns have been checked and found safe at the performance point for the predicted shear force. The columns were also tested for the shear caused by diagonal masonry struts and found safe.

Ismaeil [56] studied the seismic performance of Sudan's existing hospital buildings. Using SAP2000 software [56], the pushover analysis was approved on the building. To govern the analysis, the principles of Performance-Based Seismic Engineering are used. The assessment showed that the three-story hospital building is seismically safe.

Jarallah [57] studied the effects of the soil-structure relationship on the building's seismic assessment when a framed building is supported on a raft base. The foundation-soil interaction effect was considered by replacing it with equivalent springs. The Capacity Spectrum Method of ATC-40 [18] has been used to conduct nonlinear static pushover studies of eight-story reinforced concrete hospital buildings. The findings show that the interaction of the soil-structure has a pronounced effect on the displacement of the roof, story drift,

effective damping, and crack pattern for beams and columns while the torsional behavior of the building is minorly affected.

Jarallah et al. [58], studied the eight story RC building is the eight-story building. Using the patented software ETABS [62], the nonlinear pushover analysis of the building is predicted. The performance-based analysis has also been performed as per FEMA 356/273[21,20] and ATC40 [18]. To capture the performance level of the building, the target displacement method and the capability spectrum method were used. In the nonlinear pushover analysis, it was observed that the unreinforced masonry (URM) infills collapsed before the Maximum Considered Earthquake (MCE) performance point of the building. Whether it was possible to protect the infills by stiffening the building by having external buttresses has been explored. Two instances of retrofitting systems in the transverse direction of 1.2m wide and 3m wide buttresses were used and analyzed.

4.2.2 Review of Pushover Analysis of an Existing Other Buildings

Korkmaz et al. [59] studied the effect of infill walls on earthquake response is considered to be examined by a 3-story RC frame structure with different amounts of masonry infill walls. For modeling masonry infill walls, the diagonal strut method is adopted. For structures, pushover curves are obtained using the nonlinear analysis option of SAP2000 [60] commercial software. Besides, findings are presented and the effects of an irregular configuration of the masonry infill wall on the structural performance are presented. It was found the current study show that structural infill walls have very significant effects on structural behavior due to earthquake effects, to a large extent the global seismic behavior of framed buildings, and improved stability and integrity of reinforced concrete frames. Irregular distributions of masonry infill walls in elevation can result in unacceptably elastic displacement in the soft story frame.

Goel [61] used the non-linear static procedures set out in the documents FEMA-356 [21], ASCE/SEI 41-06 [23], ATC-40[18], and FEMA-440 [22] for the seismic analysis and assessment of building structures using strong-motion records of reinforced concrete structures. The maximum roof displacement predicted by the nonlinear static procedure is compared directly with the value derived" from the recorded movements, It is shown that: 1) for many of the buildings considered in this investigation, the nonlinear static procedures either overestimate or underestimate the peak roof displacement; 2) The ASCE/SEI 41-06 [23] Coefficient Method (CM), which is based on the recent FEMA-356 [20] (CM) proposed changes in the FEMA-440 [22] document, does not necessarily provide a better estimate of the displacement of roofs., and 3) Compared to the ATC-40 CSM, the improved FEMA-440 [22] Capacity Spectrum System (CSM) usually offers better estimates of roof displacement.

Singh et al. [62] presented an analytical review with and without Unreinforced Masonry Wall (URM) infills on the seismic performance and vulnerability (or fragility) analysis (fragility analysis of a structure is described as its susceptibility to damage by the ground shaking of a given intensity) of Indian code-designed RC frame buildings. As per ASCE 41 guidelines, infills are modeled as diagonal struts and different modes of failure are considered. The seismic vulnerability of bare and infilled frames is contrasted with nonlinear static analysis. The comparative study indicates that URM infills lead to a substantial increase in the seismic vulnerability of RC frames and that their influence needs to be better integrated into design codes.

Ahmed [63] analysed ten stories-five bays of reinforced concrete frame (two-dimensional beams and columns system) subject to the seismic risk of Mosul city/Iraq. When the member yields, the plastic hinge is used to reflect the failure mode in the beams and columns. The study of nonlinear static (Pushover) was introduced by ATC-40 [18]. The results showed that the frame is capable of resisting the presumed seismic force with many beams with some substantial yield. Only in the beams can the sequence of the creation of plastic hinges (yielding) in the frame members be seen. The building works as a weak beam mechanism with a strong column. Total overall drift, maximum inelastic drift, and structural stability do not exceed the performance level limitations, so the current building is considered safe against the seismic force for citizens.

Sabu and, Pajgade [64] focused on seismic assessment and retrofitting of existing RC buildings. Bare frame modeling, brick infill frame modeling, and soil effect interaction model are all three modeling formats. Results show that infill panels have a substantial influence on frame behavior during earthquake excitation. In general, infill panels increase the structure's stiffness, while deflection in a bare frame is very high compared to the infilled frame. The strength of the current structure can be increased to the necessary level and the building's seismic resistance capacity can be improved, the concrete jacketing method is a simple, effective, and economical way to improve the member's and building's seismic resistance capacity as well as.

Babu et al. [65] used non-linear study of different symmetric and asymmetric systems built on plain and sloping grounds subjected to different load forms. The study was carried out Using SAP2000 [60] and ETABS [66]. The paper concluded that the vertical irregularity structure is important relative to a plan irregularity structure.

Tamboli and Karadi [67] performed seismic analysis for various reinforced concrete (RC) frame construction models, including the bare frame, infilled frame, and open first Storey frame, using the Equivalent Lateral Force procedures. It examines the effects of the bare frame, infilled frame, and open first story frame, and conclusions drawn. The Equivalent Diagonal Strut system is used to model the masonry infill panels and the ETABS program [66] is used for the study of all frame models.

Golghate [68] determined the actions of the G+3 reinforced concrete frame system in Zone IV subjected to earthquake forces. The reinforced concrete structures are analyzed using SAP2000 software [60] by nonlinear static analysis (Pushover Analysis). The frame was exposed to the design of earthquake forces along the X-direction as defined. In the beams and columns showing the 3 stages of immediate occupancy, life safety, collapse prevention, the outcomes hinges have created. The column hinges have limited the damage.

Neethu and Saji [69] analyzed a symmetric construction is a portion of a four-story educational building. It was checked the type of performance that a building can provide when designed by Indian standards. The hinge length is measured as half of their effective depth for every beam and column. Using SAP2000 [60], a static non-linear (pushover) study of the current educational building was performed. The results showed that the demand curve intersects the capacity curve near the elastic range, the structure has good resistance and high collapse protection, the properly detailed behavior of reinforced concrete frame design is adequate as indicated by the demand and capacity curves intersection.

Azaz [70] used the pushover analysis on a reinforced concrete structure is emphasized in this article. In which the building of G+10 was revealed to push in x and push in the direction of y. In SAP2000 [60], the analysis was done. Nearly 6 elements exceed the limit level between life safety (LS) and collapse prevention (CP) from the results obtained in x-direction and y-direction. The study showed that the building requires retrofitting.

Daniel and John [71] studied a ten-storeyed reinforced concrete building is analyzed by displacement-controlled pushover analysis using SAP2000 software [59]. It was developed to model the beam and column sections of the user-defined hinges. The lateral forces were connected to the building. Pushover analysis is carried out in the direction of +x and +y by vertical loading (gravity load) followed by a gradually increasing displacement-controlled lateral load. The results showed that the maximum base shear capacity was greater than the base shear design, and the hinge formation sequence showed that localized collapse occurs before columns in beams.

Sangeetha and, Sathyapyiya [72] analyzed a four-story building construction is planned and evaluated according to the Indian standard in the report. Structural analysis and design software SAP 2000 [60] conducts the pushover analysis of the RC building frame. The frame was subjected to the X-directions of design earthquake forces. In the beams and columns showing the 3 stages of immediate occupancy, life safety, collapse prevention, the results showed that hinges have grown. The damage has been limited by the column hinges. It proposed some retrofitting, buckled longitudinal reinforcement, broken ties, and crushed concrete by replacing new reinforcement welded with existing bars and supplying new additional closed ties.

Ning, N.et al. [73] presented a pushover study using ABAQUS. The influence of the infills on the RC frames' failure patterns was studied. An RC frame with completed infills, half-filled infills, and without infills is considered to be the Finite Element Method (FEM) model. Research findings suggest that because of the influence of infills, the position of the inflection point differed. The effective slab width and the required ratio of a column to beam strength are found to be reduced due to the infill effects. The actual effective width of the slab should be considered in the required ratio of a column to beam strength.

Cavdar et al. [74] studied a building that collapsed in the Turkish earthquake in 2003; pushover analysis and nonlinear dynamic analysis were carried out. To test the reliability and usability of performance levels, their purpose was to perform the pushover analysis and NDA for various earthquakes. The present Turkish Earthquake Code, TEC (2007) [46] was used to conduct a performance assessment. It is concluded that when a reinforced-concrete shear-wall building is not severely damaged, pushover will provide a fairly reliable measurement of performance level. Pushover analysis underestimates the building efficiency, regardless of the lateral load distributions, if the building is severely collapsed.

Al-jassim and Husssain [75] used a nonlinear static analysis (Pushover analysis based on the ATC40 capacity spectrum approach to analyze an existing G + 5 story reinforced concrete building. In three instances, the building is evaluated (regular, irregular in plan, and irregular in height). The default plastic hinge in the SAP2000 program [60] is built. Results clearly illustrate that during the design earthquake, all buildings perform very well (nearly elastic), which means that the buildings are over-designed. At an output level below the immediate occupancy level, all the plastic hinges are both buildings behave almost elastically, with no noticeable difference between their activities, except that the irregular plan building shows less Y-direction displacements and drifts than the other buildings.

Abhilash and Vijayanand [76] carried out pushover analysis by using ETABS software [65] to understand the conduct of G+8 multistoried building in two separate areas in India. From the results of the study, maximum lateral load, story displacement, and monitored displacement were found to be increased in Zone III compared to Zone II. Although in Zone II, the maximum base force is higher than in Zone III. The hinges between IO (Immediate Occupancy) and LS (Life Safety) are established here, indicating the building. Hence the structural model analyzed in this state is safe.

Ingale and Kalurkar [77], studied the effect of Push over analysis for G+15 story RC structure with and without the Zipper frame using SAP2000 [60] software. For the rising efficiency of RC, Framed structure types of bracing systems, such as zipper braced frame, are used in framed structures for seismic design. The displacement values for regular RC construction (without the zipper brace frame) were found to increase compared to the zipper brace frame displacement. The pushover analyses are helping to understand the model behavior and its demand as well as capacity as shown in the above results.

5. Torsional Effects in Pushover Analysis

Studies on the torsion effects of irregular buildings date back to the 30s of the last century [78]. There can be several and varying types of causes of irregularity in a building configuration and they are usually classified into two key categories: plan and elevation irregularities [79]. Among the two aforementioned types of structural irregularity, in-plan irregularity appears to have the most adverse effects on the applicability of classical nonlinear static procedures (NSPs), precisely because such methods have been developed for seismic assessment of structures whose activity is primarily translational [80]. This explains why the improvement of NSPs in recent years has centered mainly on the contribution of higher vibration modes, which are intended to account for the effects of vertical and in-plan irregularities. Two main approaches can be identified among the many proposed methods developed in this research field: the first one aims to take into account the contribution of more eigen modes called model pushover analysis (MPA), in addition, a similar approach, an extended version of the N2 method has been proposed by Fajfar et al. [81] for the application to plan irregular building structures.

5.1 Analytical techniques of torsional effect in pushover analysis

5.1.1 Model Pushover Analysis (MPA)

One of the main approaches in the developing of NSPs for the analysis of irregular building structures involves the evaluation of the contribution of more Eigen modes in the analysis. Within this approach, the major contribution has been given by Chopra and Goel [82] who extended the previously defined MPA to asymmetric-plan buildings.

5.1.1.1 Brief Description of MPA Procedures [83]

To better understand the method proposed in this research, it is summarized below:

1. Compute the structural natural frequencies ω_n and modes Φ_n. In practical applications, only the first two or three modes are needed.

2. For the nth mode, develop the pushover curve (base shear-top displacement curve) using force distribution s_n^* defined as

$$s_n^* = M\varphi_n \qquad \text{....... (63)}$$

where M is the mass matrix of the structure.

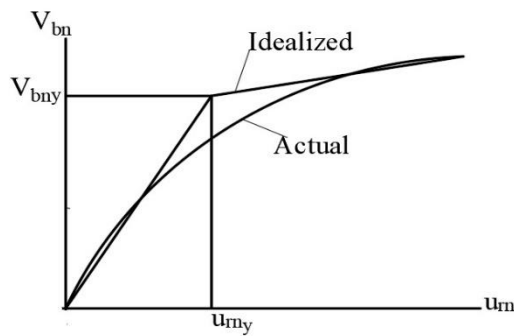3. Idealize the pushover curve as a bilinear curve as shown in Fig.15.

Figure (15): Pushover curve and the idealized bilinear curve

4. Convert the idealized pushover curve to the force-deformation relationship (F_{sn}/L_n -D) of nth mode inelastic SDF system as shown in Fig.16.

$$\frac{F_{sn}}{L_n} = \frac{V_{bn}}{M_n^*}, D_n = \frac{u_{rn}}{\Gamma_n\varphi_m}, M_n^* = L_n\Gamma_n \quad \dots (64)$$

where Γ_n is the nth modal participation factor, and M_n^* is the effective modal mass and determine the initial elastic vibration period T_n and yielding deformation D_{ny}.
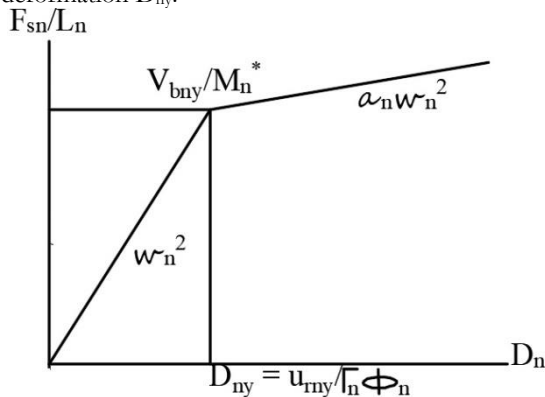

Figure (16): Converted force-displacement relationship for equivalent SDF system.

5. Compute the peak deformation D_n of the nth mode inelastic SDF system by nonlinear history analysis, or using inelastic design spectrum.

6. Calculate the peak roof displacement u_{rn} associated with the nth-mode inelastic SDF system from

$$u_{rn} = \Gamma_n\varphi_{rm}D_n \quad \dots (65)$$

7. From the pushover database, extract values of any desired responses r_n at the peak roof displacement u_{rn}.

8. Repeat steps 3-7 for the first few "modes".

9. Determine the total seismic demand r_{total} with Square Root of Sum of Squares (SRSS) rule

$$r_{total} = \sqrt{\sum r_n^2} \quad \dots (66)$$

5.1.2 Extended N2 Method

The extension to plan-asymmetric buildings of the N2 method, where torsional effects are significant, it was established by assuming that the torsional effects in the inelastic range are Just like in the elastic range, the torsional effects are determined by the standard elastic modal analysis. The displacements taken by pushover analysis are amplified through a corrective factor, given by the ratio of the normalized displacement gained by modal analysis and that incoming from pushover analysis. It is assumed that the structure stays in the elastic range when vibrating in higher modes, and

that the seismic demands can be calculated as an envelope of demands determined by a pushover analysis, which does not take into account the higher mode effects, and normalized demands determined by an elastic modal analysis, which involves higher mode effects [84].

5.1.2.1 Brief Description of Extended N2 Procedures [85]

The following procedure can be applied to predict the structural response for a building with a non-negligible effect of higher modes along the elevation:

1. Perform the basic N2 analysis and find out the target roof displacement.

2. Perform the standard elastic modal analysis of the MDOF model considering all relevant modes. Identify floor drifts for each floor. Normalize the results in such a way that the top displacement is equal to the target top displacement.

3. Determine the envelope of the results obtained in Steps 1 and 2.

4. For each floor, determine the correction factor C_{HM}, which are defined as the ratio between the results obtained by elastic modal analysis (Step 2) and the results obtained by pushover analysis (Step 1). If the ratio is larger than 1.0, the correction factor C_{HM} is equal to this ratio, otherwise it amounts to 1.0. The correction factors for storey drifts are important.

5. The resulting floor drifts (and displacements, if applicable) are obtained by multiplying the results determined in Step 1 with the corresponding correction factors C_{HM}.

6. Determine other local amounts. The resulting correction factors for floor drifts CHM apply to all local deformation amounts (e.g. rotations). Correction factors C_{HM} for floor drifts also apply to internal member forces, provided that the resulting internal forces do not exceed the load-bearing capacity of the structural member.

5.2 Criteria of Seismic Codes on Applicability of NSPs to Torsional Effects

In spite of the large tries of researchers to better understand the seismic behavior of irregular building structures and to improve the current NSPs, it appears that most regulatory forms have not still translated the research improvements achieved into seismic codes.

ASCE7-10 [86] specific prescriptions for the use of NSPs are not included. The only constraint on the option of the form of study with respect to torsional irregularity is that similar lateral force analysis is not required for torsionally irregular structures.

ASCE 41-06 [23] defines limitations in the use of linear analyses centered on the presence of structural irregularities evaluated by static or dynamic linear analysis. If there is some form of structural irregularity (in-plane and out-of-plane discontinuities, weak story, torsional strength/stiffness irregularity) defined by one or more structural components, then linear procedures are not applicable and should not be used.

FEMA 273 [20] It advises that the effects of torsion cannot be used to reduce the demands on

components and elements for force and deformation.

EC8-1 [24] provides for the application of the N2 method, although it meets the absence of a full suitability for irregular building structures.

Japanese Guidelines [25] provides a numerical method to take the irregular building effects in to account by using the factor SD in seismic index.

6. Acceptance Criteria

Response quantities from the nonlinear static analysis are compared with limits for acceptable performance levels to decide whether a building meets a specified performance level. The limits of response fall into two groups [18]:

1. Global building acceptability limits: These response limits include requirements for the vertical load capacity, lateral load resistance, and lateral drift.

2. Element and component acceptability limits: Each element (frame, wall, diaphragm, or foundation) must be checked to determine if its components respond within acceptable limits.

6.1 Global building acceptability limits

Lateral deformations at the performance point displacement are to be checked against the deformation limits. Deformation limits for various performance levels and for various seismic assessment codes were presented below.

6.1.1 ATC-40[18]

Table (7): Limits of global building according to ATC-40[18]

Inter-story Drift Limit	Immediate Occupancy	Life Safety	Structural Stability
Maximum Total drift	0.01	0.02	$0.33V_i/P_i$
Maximum Inelastic drift	0.005	No limit	No limit

6.1.2 Japanese Standard [25]

Seismic index of the structure for each story
$$I_s = E_o.S_D.T$$

Seismic demand index(Iso) regardless of the number of stories in the building:
$$I_{so} = E_s.Z.G.U$$

$$\text{If } I_s \geq I_{so} \quad \ldots\ldots\ldots (63)$$

If eq.63 was fulfilled, the building is safe. If eq.63 was not fulfilled, the building is unsafe and it needs to retrofit

6.1.3 TEC-2007[46]

Table (8): Boundaries of Relative Story Drift according to TEC-2007

Ratio of Relative Story Drift	Damage Boundary		
	MN[1]	GV[2]	GC[3]
δ_{ji}/ h_{ji}[4]	0.01	0.03	0.04

1. MN is Minimum Damage Region.
2. GV is Safety Limit.
3. GC is Collapsing Limit.
4. δji / hji4, δji The relative drift of the story is measured as a substitute difference between the bottom and top ends of the jth column or wall in the ith storey, while hji indicates the height of the related element.

Table (9): Performance criteria used in analyses (TEC-2007)

Damage Level	Limited value for confined concrete	Limited values for steel bar
Minimum Damage Limit (MN)	$(\varepsilon_{cu})MN$ =0.0035	$(\varepsilon_s)MN$ =0.010
Safety Damage Limit (GV)	$(\varepsilon_{cg})_{cv}$ $= 0.0035$ $+ 0.01(\rho_s/\rho_{sm})$ ≤ 0.0135	$(\varepsilon_s)GV=0.040$
Collapse Damage Limit (GC)	$(\varepsilon_{cg})_{GC}$ $= 0.004$ $+ 0.014(\rho_s /\rho_{sm}) \leq 0.018$	$\varepsilon_s)GC=0.060$

6.1.4 TEC-2018[87]

Table (10): Performance criteria used in analyses (TEC-2018)

Damage Level	Limit Values	
	Confined Concrete	Steel Bar
Limited Damage (SH) Boundary	$(\varepsilon_c)^{SH} = 0.0025$	$(\varepsilon_s)^{SH}$ $= 0.0075$
Controlled Damage (KH) Boundary	$(\varepsilon_c)^{KH}$ $= 0.75(\varepsilon_c)^{GO}$	$(\varepsilon_s)^{KM}$ $= 0.75(\varepsilon_{su})^{GO}$
Collapse Prevention (GO) Boundary	$(\varepsilon_c)^{G0}$ $= 0.0035$ $+ 0.04\sqrt{w_e}$ ≤ 0.018	$(\varepsilon_s)^{60}$ $= 0.40\varepsilon_{su}$

6.2 Element and component acceptability limits

To determine if its components meet acceptability criteria under performance point forces and deformations, each part must be examined. Primary and secondary elements and provides general information on checks for strength and deformability. Each element and component is classified as primary or secondary, depending on its importance at or near the performance point for the lateral load resisting system. Plastic hinge properties can be characterized by a typical elastic-plastic force-deformation relationship with strength degradation at high ductility demands as shown in Fig.17.
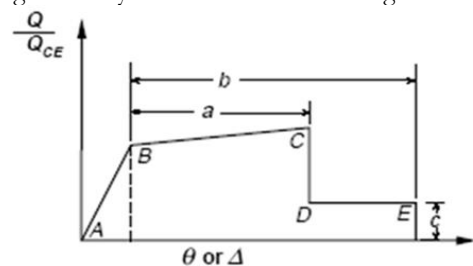

Figure (17): Component modeling and acceptability.

Point A identify to the unloaded condition; Point B has a resistance equal to the nominal yield strength, taken as 10% total strain hardening for steel, the abscissa at C identify to the deformation at which considerable strength degradation begins, point defining the maximum deformation capacity [88].

6.2.1 Review of plastic hinge properties in nonlinear analysis

Inel and Ozmen [89] studied the effect of default and user-defined nonlinear component properties in the results of pushover analysis. For this analysis, four- and seven-story structures were observed to reflect low- and medium-rise buildings. Pushover analysis is carried out in many programs based on the FEMA-356[21] and ATC-40[18] guidelines for either user-defined nonlinear hinge properties or default-hinge properties. Observations show that the length of the plastic hinge and the spacing of the transverse reinforcement have little effect on the base shear capacity, while these parameters have a significant impact on the frame displacement capacity.

Eslami and Ronagh [90] demonstrated the effects of pushover studies of modeled RC structures based on the nonlinear FEMA hinges and identified hinges. The force-deformation curves of the specified hinges are calculated following the validation of the adopted models in a rigorous approach taking into account the material inelastic behavior, reinforcement details, and members' dimensions. Concerning the inter-story drift, hinging pattern, failure mechanism, and the pushover curve, nonlinear responses of both models are elaborated. FEMA hinges have been confirmed to underestimate the strength and more importantly, the displacement capacity, especially for frames with low ductility.

Jadhav and Patil [91] studied the variations in pushover analysis results by reason SAP2000 [59] default and user-defined hinge properties. The amount of transverse reinforcement is the parameter assumed to affect the frame's base shear ability and displacement capacity. The comparison points out that the displacement capacity is increased by a raise in the quantity of transverse reinforcement. But because it takes average values, the capacity curve for the default hinge model is reasonable. Compassion demonstrates that the user-defined hinge model is better at capturing the hinge mechanism than the default hinge model. However, the default hinge model is preferred due to simplicity but the user should be aware of what is provided in the program.

LOPEZ et al. [92], studied the influence on the nonlinear behavior of reinforced concrete structures of various plastic hinge models. Considering the FEMA-356[21] plastic hinge model and two additional models, several nonlinear analyses were carried out using empirical expressions calibrated with different experimental data. The results show that plastic hinges modeled with empirical expressions can be used to model the behavior of structural components more precisely, besides, to

compare the results of the models included in seismic building design codes.

7. Seismic Retrofit

The strengthening and enhancement of the performance of deficient structural elements in a structure or the structure as a whole is referred to as retrofitting. Retrofitting of a building is not the same as repair or rehabilitation. Repair refers to the partial improvement of the degraded strength of a building after an earthquake [93]. The approaches considered for the existing buildings such as Jacketing of existing beams, columns. Several authors carried out numerical and experimental campaigns on the behavior of concrete structural elements before and after the Carbon Fiber Reinforced Polymer (CFRP) wrapping [94]. Another retrofitting technique is steel bracing, Steel Bracings Systems modify the structural response in seismic or collapse scenarios maintaining the before mentioned advantages and reducing the cost [95].

7.1 Retrofitting of Existing Buildings under Seismic Loading

Fahmi and, Faraj [96] concerned with the seismic evaluation of existing reinforced concrete buildings. The methodology includes linear elastic analysis based on equivalent static lateral load according to the 1988 Uniform Building Code and the Draft Iraqi Seismic Code. Six-story moment-resisting frame structure with shear wall located in Baghdad. The results indicate that the stress ratio of some members (beams, columns) of the existing building are determined using the stresses due to the vertical and seismic forces divided by the allowable stresses more than one. These critical elements are inadequate and need strengthening. The mechanism of strengthening by using shotcrete and reinforcement on the outside of the original cross-sectional area of the element. The stress ratio indicates that after strengthening each element in the existing building has adequate strength to resist the vertical and seismic forces.

Dhiman et al. [97] studied the response of a braced and unbraced structure subjected to seismic loads was evaluated and the appropriate bracing system was identified to effectively resist seismic loads. After analyzing the structure with different types of structural systems, it was concluded that after the application of the bracing system, the displacement of the structure decreases. The maximum reduction in lateral displacement occurs after the cross-bracing system has been applied. In the columns, the bracing system decreases bending moments and shear forces. The lateral load is transferred through axial action to the foundation. The cross-bracing system performance is better than the other bracing systems specified, Steel bracings can be used to retrofit the existing structure. The total weight of the existing structure will not change significantly after the application of the bracings.

Bhojkar and Bagade [98] analyzed reinforced concrete (RC) structures with different bracing types are studied in this paper. By using STAAD Pro software [99], a G+9 building is analyzed. In this paper, lateral displacement, story drift, axial force,

base shear are the main parameters considered to compare the seismic analysis of buildings. The X type of steel bracing has been found to significantly contribute to the structural stiffness and reduce the maximum inter-story drift of the frames. The bracing system improves not only the lateral stiffness and strength capacity but also the displacement capacity of the structure.

Hyderuddin et al. [100] investigated the seismic efficiency of reinforced concrete (RC) buildings rehabilitated using concentrated steel bracing. For peripheral columns, bracing is provided. By using ETABS 2015 [62] Software, a ten-story building is analyzed. For models with Diagonal bracing,' V' form bracing, inverted 'V' form bracing, inverted 'V' form bracing,' X' form bracing,' K' form bracing, the design is evaluated and compared to an unbraced frame bracing. Lateral displacement, story drift, axial forces in the columns, base shear are the main parameters in this study to compare the seismic analysis of buildings. It was found that the 'X' type of steel bracing contributes greatly to the structural stiffness and decreases the frames' overall story drifts. The bracing systems increase not only the lateral stiffness but also the structure's displacement strength.

Basereh et al. [100] introduced a new retrofit method for code-deficient reinforced concrete shear walls which, due to improper detailing or lack of well-confined boundary elements, are vulnerable to non-ductile failure modes. To define working specifics of the retrofit process, three-dimensional finite element models of pre-and post-retrofit shear walls under cyclic lateral loading have been used. Results of the analysis showed that rocking is the governing behavior for the retrofitted walls and the contribution of shear to displacements decreased due to retrofit. Changes in residual displacements, energy dissipation, strength, and secant stiffness due to retrofit were documented.

8. Conclusions

From the previous review on evaluation and retrofitting of an existing building and their procedures, it can be noted that the researcher aimed to investigate the behavior of buildings under seismic loads, assess the level of an existing building state under loads, in addition, retrofitting the weak links in an existing building. From literature, the following prominent remarks concerning the seismic evaluation and retrofit of buildings:

1. The improvement of capacity spectrum method (CSM) and displacement coefficient method (DCM) in FEMA 440 focused on the effect of stiffness degradation and changes in dynamic properties associated with progressive damage but doesn't take the effect of irregularity in plan or in elevation into account, on the other hand the Japan Standard relied on a numerical method taking the stiffness degradation and the torsional effect in the seismic evaluation.

2. ATC-40, FEMA273/356, FEMA440, and ASCI 41-06 are considered the most important than Euro code 8 – Part 3 and Italian Seismic Code,

Italian seismic code and EC8 do not consider the dynamic P-Δ effects. Also, according to FEMA440, the procedures implemented in FEMA273/356 and ATC-40 are not able to adequately capture the dynamic instability phenomenon.

3. Nonlinear static analysis (Pushover analysis) Procedures are deemed to be a very practical tool to assess the nonlinear seismic performance of structures, it introduced in this context are a powerful tool for performance evaluation.

4. Unreinforced Masonry Wall (URM) infills have a significant increase in the seismic vulnerability of RC frames compare with the bare frame and their effect needs to be properly incorporated in design codes.

5. The soil-structure interaction has a marked effect on the global acceptability limits as a roof displacement and story drift. Most researchers don't take this effect into account.

6. For SAP2000 and ETAPS, the user-defined hinge model is better than the default hinge model in displaying nonlinear behavior consistent with element properties.

7. Despite the large efforts of researchers aimed at the improvement of NSPs for a reliable application to irregular buildings, these developments have not yet transposed to Both European and American codes. For this reason, these cods are still in need of improvement regarding specific prescriptions concerning the seismic analysis of irregular structures.

8. The retrofitting by adding steel braces enhance greatly the strength capacity of the buildings on the dynamic characteristic of the building. The zipper (vertical structural member, connected at the top and down to the beams at the vertical strut) bracing systems are found the most efficient.

Abbreviations

A list of symbols should be inserted before the references if such a list is needed

CSM	Capacity Spectrum Method.
DCM	Displacement Coefficient Method.
T_e	Effective fundamental period of the building in the direction under consideration.
T_i	Elastic fundamental period (in seconds) in the direction under consideration calculated by elastic dynamic analysis.
K_i	Elastic lateral stiffness of the building in the direction under consideration
K_e	Effective lateral stiffness of the building in the direction under consideration.
T_S	Characteristic period of the response spectrum, defined as the period associated with the transition from the constant acceleration segment of the spectrum to the constant velocity segment of the spectrum.

R	Ratio of elastic strength demand to calculated yield strength coefficient.
S_a	Response spectrum acceleration.
S_1	Response spectrum acceleration at period,1 sec.
V_y	Yield strength calculated using results of the NSP for the idealized nonlinear force-displacement curve developed for the building.
W	Effective seismic weight.
C_m	Effective mass factor.
α	The ratio of post yield stiffness to elastic stiffness when the nonlinear force-displacement relation is characterized by a bilinear relation.
α_e	Effective negative post-yield slope ratio.
$\alpha_{p-\Delta}$	Negative slope ratio caused by P-Δ effects.
λ	Near field effect factor.
PF1	Modal participation factor for the first natural mode.
α_1	Modal mass coefficient for the first natural mode.
V	Base shear.
Δ_{roof}	Roof displacement (V and the associated Δ_{roof} make up points on the capacity curve).
β_{eq}	Equivalent viscous damping.
β_{eff}	Effective viscous damping.
k	Damping modification factor
β_1	Hysteretic damping represented as equivalent viscous damping.
E_D	Energy dissipated by damping.
E_{S0}	Maximum strain energy.
E_{S0}	Maximum strain energy.
SR_A	Spectral Acceleration Reduction.
SR_v	Spectral Velocity Reduction.
T*	Elastic Period.
R_μ	Reducing Factor.
Tc	Characteristic Period.
α_2	Negative post-yield slope ratio.
Δ_d	Displacement at maximum base shear.
Δ_y	Displacement at effective yield strength.
T_{eff}	Effective period.
μ	Ductility factor.
β_{eff}	Effective damping.
β_0	Initial viscous damping (5% - concrete buildings).
T_0	Fundamental period in the direction under consideration.
a_{pi}	Trail Spectral Acceleration.
d_{pi}	Trail Spectral Displacement.
a_y	Bilinear curve yielding spectral Acceleration.
d_y	Bilinear curve yielding spectral Displacement.

d_y	Bilinear curve yielding spectral Displacement.
SDOF	Single Degree of Freedom.
MDOF	Multi Degree of Freedom.
RC	Reinforcement Concrete.
ATC	Applied Technology Council.
FEMA	Federal Emergency Management Agent.
ASCI	American Society of Civil Engineers.
EC	Euro Code.
IO	Immediate Occupancy.
LS	Life Safety.
CP	Collapse Prevention.

9. References

[1] G. G. Deierlein, A. M. Reinhorn and M. Willford (2010), "Non-Linear Structural Analysis for Seismic Design, A guide for practicing engineer", National Institute of Standards and Technology NEHRP Seismic Design Technical Brief No. 4, Gaithersburg, MD, USA.

[2] S. E. Abdel Raheem and T. Hayashikawa (2003), "Nonlinear behavior of cable-stayed bridges tower under level II earthquake ground motion", International Workshop on Structural Health Monitoring of Bridges/Colloquium on Bridge Vibration, Kitami, Hokkaido, Japan.

[3] A. Mechaala, C.Benazouz, H. Zedira, and M. Benbouras (2018), "Evaluation of the displacement coefficient method for seismic demands assessment of structures", 14th ASEC conference in Jordan 12-15 April 2018 Jordan University of Science &Technology.

[4] A. Bagchi (2001), "Evaluation of The Seismic Performance of Reinforced Concrete Buildings", Ph.D., dissertation to Civil and Environmental Engineering, Carleton University, Ottawa, Canada.

[5] H. He, M. Cong, and Y. Lv (2013), "Earthquake Damage Assessment for RC Structures Based on Fuzzy Sets", Mathematical Problems in Engineering, Hindawi Publishing Corporation, Article ID 254865.

[6] R. Dumaru (2018), "Seismic Performance Assessment and Strengthening Techniques for Existing Reinforced Concrete in Nepal", Ph.D., dissertation to the Faculty of Engineering of the University of Porto, Portuguese public.

[7] A. Biddah, A. Ghobarah and H. ABOU-ELFATH (2000), "Response Based Damage Assessment of Structures", Earthquake Eng. Struct. Dyn. 28, 79-104.

[8] A. Ghobarah (2004), "On drift limits associated with different damage levels", M.Sc., thesis submitted to the Department of Civil Engineering, McMaster University, Hamilton, Canada.

[9] E. Erduran and A. Yakut (2004), "Drift Based Damage Functions for Components of RC Structures", 13th World Conference on Earthquake Engineering, Vancouver, B.C., Canada.

[10] M. Seckin (1981), "Hysteretic behavior of cast-in-place exterior beam-column sub-assembles", Ph. D. Thesis, University of Toronto, 266 pp, Canada.

[11] S.Okamoto, S. Shiomi and K. Yamabe, (1976), "Earthquake Resistance of Prestressed Concrete Structures", Proceedings, Annual Convention, pp. 647-665.

[12] B. P. Sinha, K. H. Gerstle, and G. T. Leonard (1964), "Stress-Strain Relations for Concrete under Cyclic Loading", ACI Journal, Proceedings, Vol.61, No.2, pp. 195-212.

[13] P. Fajfar, T. Vidic and M. Fischinger (1992), "On energy demand and supply in SDOF systems, "Nonlinear seismic analysis and design of reinforced concrete buildings", pp 41-62.

[14] G. Manfredi (2001), "Evaluation of seismic energy demand", Earthquake Engng Struct. Dyn. : 30:485–499.

[15] H. Park and T. Eom (2004), "Energy dissipation capacity of flexure-dominated RC members", 13th World Conference on Earthquake Engineering, Vancouver, B.C., Canada, Paper No. 3481.

[16] C. Negulescu and, K. K. Wijesundara (2019), "Energy-based seismic design: Needs of Energy Damage Index Values for Serviceability and the Ultimate Limit States for Gravity Design Buildings?" 13th World Conference on Earthquake Engineering At: Crete, Greece, DOI:10.7712/120119.7079.19379.

[17] B. Yön, E. Sayın and O. Onat (2017), "Earthquakes and Structural Damages", Earthquakes - Tectonics, Hazard and Risk Mitigation, DOI: 10.5772/65425.

[18] Applied Technology Council, 1996, "Seismic Evaluation and Retrofit of Concrete Buildings", Report No. SSC 9601: ATC-40, Vol.1, Redwood City, California.

[19] Fajfar. A nonlinear analysis method for performance-based seismic design. Earthquake Spectra . 2000, Vol. 16(3), pp. 573-592.

[20] Federal Emergency Management Agency, 1997, "NEHRP Guidelines for the Seismic Rehabilitation of Buildings", FEMA-273", Washington, D.C.

[21] Federal Emergency Management Agency, 2000, "Prestandard and Commentary for the Seismic Rehabilitation of Buildings", FEMA-356, Washington, D.C.

[22] ATC, Applied Technology Council. "Improvement of Nonlinear Static Seismic Analysis Procedures", FEMA440 Report. Redwood City, CA, 2005.

[23] ASCE, Seismic analysis of safety-related nuclear structures and commentary. ASCE standard no.004-98, American Society of Civil Engineering, 2000.

[24] CEN (2005a), EN 1998-3 Eurocode 8; "Design of structures for earthquake resistance, part 3: assessment and retrofitting of buildings", European Committee for standardization.

[25] The Japan Building Disaster Prevention Association (JBDPA), "Standard for Seismic Evaluation of Existing Reinforced Concrete Buildings" (JBDPA, Tokyo, 2001).

[26] NZS1170.5. "Structural Design Actions Part 5: Earthquake Actions – New Zealand", Standards New Zealand, 2004.

[27] Seismic evaluation and strengthening of existing reinforced concrete building - Guidelines, IS 15988 (2013), Bureau of Indian Standards, New Delhi.

[28] B. Mahaylov, and L. Petrini (2006), "Analysis of Code Procedures for Seismic Assessment of Existing Buildings: ITALIAN Seismic Code, EC8, ATC-40, FEMA356, FEMA440", Ph. D. Thesis, University of Pavia, Italy.

[29] Italian Ministry of Public Works, Ministry Decree. 14/01/2008. Technical Regulations for Constructions; Suppl. Ord. Gazzetta Ufficiale n. 29, 4/02/2008; Istituto Poligrafico e Zecca dello Stato: Rome, Italy, 2008. (In Italian).

[30] A. Moshref, S. M. Moghaddasi and Tehranizadeh, M. (2011), "Comparison of Different Non-Linear Static Analysis Used for Seismic Assessment of Existing Buildings", COMPDYN 2011 III ECCOMAS Thematic Conference on Computational Methods in Structural Dynamics and Earthquake Engineering, Greece.

[31] New Zealand National Society for Earthquake Engineering (NZSEE) (2002), "The Assessment and Improvement of the Structural Performance of Earthquake Risk Buildings", NZSEE 2002, Draft Prepared for the NZ Building Industry Authority

[32] H. Alwashali, and M. Maeda (2012), "Study of Low-Rise RC Buildings with Relatively High Seismic Damaged by Great East JAPAN Earthquakes 2011", Conference: Proceedings of Japan Concrete Institute at Japan Volume: Vol 34, No.2, pp.1147-1152.

[33] C. Xiaoguang, B. Jingshan, S. Youwei, and Z. Jianyi (2012), "Comparison of Seismic Fortification Criterion of Eight Asian Countries", 15th World Conference on Earthquake Engineering At Lisbon, Portugal 2012.

[34] Earthquake resistant design for buildings (2001). Japan, Ministry of Land, Infrastructure and Transport, 82-102.

[35] Criteria for earthquake design of structures -Part 1 general provisions and buildings (2001). India, IS 1893-2002 Indian standard, 1-35.

[36] Specification for structures to be built in disaster areas (1998). Turkey, Ministry of public works and settlement, 1-32.

[37] Seismic Design of Buildings application and analysis (GB 50011-2010) (Chinese Edition) Paperback – January 1, 2000

[38] Building code for structural regulations (1988). Korea, Ministry of construction and transportation, 1-18.

[39] NBC105 Nepal national building code, Seismic design of buildings in Nepal (1995). Nepal, Ministry of housing and physical planning, 1-31.

[40] SNI-02-1726-2002, Seismic resistance design

standard for buildings (2002). Indonesia, Ministry of public work, 1-25.

[41] Iranian code for seismic resistant design of buildings (1988). Iran, Building and housing research center, 1-49.

[42] M. Araújo, J. M. Castro, X. Romão and R. Delgado (2012), "Comparative Study of the European and American Seismic Safety Assessment Procedures for Existing Steel Buildings", 15th World Conference on Earthquake Engineering At Lisbon, Portugal 2012.

[43] R. A. Hakim, M. S. Alama and S. A. Ashour (2014), "Seismic Assessment of RC Building According to ATC 40, FEMA356 and FEMA 440", Arab J Sci Eng (2014) 39:7691–7699 DOI 10.1007/s13369-014-1395-x

[44] The Saudi Building Code 301 Structural Loading and Forces, the Saudi Code National Building Committee (2007).

[45] O. Cavdar, and, A. Bayraktar (2013) , "Pushover and nonlinear time history analysis evaluation of an RC building collapsed during the Van (Turkey) earthquake on October 23, 2011", Nat Hazards (2014) 70:657–673. DOI 10.1007/s11069-013-0835-3.5.

[46] Ministry of Public Works and Settlement. Provisions for structures to be built in disaster areas. Ankara (Turkey); 2007.

[47] Ministry of Public Works and Settlement. Provisions for structures to be built in disaster areas. Ankara (Turkey); 1975.

[48] A. Kurniawandy and S. Nakazawa (2019), "Seismic performance evaluation of existing building using Seismic Index method", MATEC Web of Conferences 276, 01015.

[49] R. Lewandowski and P. Wielentejczyk (2019), "Analysis of dynamic characteristics of viscoelastic frame structures", Archive of Applied Mechanics, DOI: 10.1007/s00419-019-01602-4.

[50] P. Fajfar (2000), "A Nonlinear Analysis Method for Performance-Based Seismic Design", Earthquake Spectra, 16:573-592.

[51] D.G. Lee, W.H. Choi, M.C. Cheong, and D.K. Kim, (2006), "Evaluation of Seismic Performance of Multistory Building Structures Based on the Equivalent Responses", Engineering Structure, 28:837-856.

[52] G. D. Seneviratna, and H. Krawinkler (1997), "Evaluation of Inelastic MDOF Effects for Seismic Design", John A. Blume Earthquake Engineering Center, Standford University.

[53] S. A. Freeman (2004), "Review of the Development of the Capacity Spectrum Method", ISET Journal of Earthquake Technology, Paper No. 438, Vol. 41, No. 1, pp. 1-13.

[54] M. Al Telbani (2015), "Seismic Resistance of Reinforced Concrete Buildings Designed for Gravity Loads in Gaza Strip", M.Sc., thesis submitted to Civil Engineering Department, The Islamic University – Gaza

[55] Y. Singh, H.K. Jarallah, and D. K. Paul, (2006),

[56] "Seismic evaluation of ward blocks GTP hospital", Technical Report No. EQ: 2006-10, Department of Earthquake Engineering, Indian Institute of Technology Roorkee, India. 69p.

[56] M. Ismaeil (2014), "Pushover Analysis of Existing 3 Stories RC Flat slab Building", International Journal of Advances in Science and Technology (IJAST), ISSN: 2348-5426.

[57] H. K. Jarallah (2015), "Effect of Soil-Structure Interaction on Seismic Evaluation of Existing Building Frames Resting on Raft Foundation", Basrah Journal for Engineering Sciences, vol. 15, no. 1.

[58] H. K. Jarallah, D. K. Paul and Y. Singh, (2020), "Seismic Evaluation and Retrofitting of an Existing Hospital Buildings", Journal of Engineering and Sustainable Development, ISSN: 2520-0917, Vol. 24 No. 06.

[59] K. A. KORKMAZ, F. DEMİR, and M. SİVRİ (2007), "Earthquake Assessment of R/C Structures with Masonry Infill Walls", International Journal of Science & Technology, Volume 2, No 2, 155-164.

[60] Computers and Structures, SAP2000 v12 Integrated finite element analysis and design of structure basic analysis reference manual, (2012).

[61] R. Goel, (2008), "Evaluation of current nonlinear static procedures for reinforced concrete buildings", 14th World Conference on Earthquake Engineering, Beijing, China.

[62] Y. Singh, P. Haldar and D. K. Paul (2012), "Effect of URM infill on the seismic vulnerability of Indian code designed RC frame buildings", Earthq Eng & Eng Vib. 11: 233-241, Vol.11, No.2, DOI: 10.1007/s11803-012-0113-5.

[63] S. Y. Ahmed (2013), "Seismic Evaluation of Reinforced Concrete Frames Using Pushover Analysis", Al-Rafidain Engineering, Vol.21 No.3.

[64] D. Sabu and, P. Pajgade (2012), "Seismic Evaluation of Existing Reinforced Concrete Building", International Journal of Science & Technology, ISSN Online 2229-5518, PP.1408-1415.

[65] N. J. Babu, K. V. Balaji and S. S. GopalaRaju, (2012), "Pushover Analysis of Unsymmetrical Framed Structures on Sloping Ground", International Journal of Civil, Structural, Environmental and Infrastructure Engineering, ISSN 2249-6866 Vol. 2.

[66] ETABS plus Version 9.7.1, "Extended 3-D Analysis of Building Systems", Computer and Structures, Inc., Berkeley, CA, USA

[67] H. R. Tamboli and U. N. Karadi (2012), "Seismic Analysis of RC Frame Structure with and without Masonry Infill Walls", Indian Journal Of Natural Sciences (IJONS), ISSN: 0976 – 0997, Vol.3.

[68] K. Golghate (2013), "Pushover Analysis of 4 Storey's Reinforced Concrete Building", International Journal of Latest Trends in Engineering and Technology (IJLTET), ISSN: 2278-621X, Vol. 2 Issue 3.

[69] N. Neethuand K. Saji, (2013), "Pushover Analysis of RC Building", International Journal

of Science and Research (IJSR), ISSN (Online): 2319-7064., Index Copernicus Value: 6.14 | Impact Factor (2013): 4.438.

[70] M. Azaz (2015), "Pushover Analysis on G+10 Reinforced Concrete Structure for zone II and Zone III Ad Per IS 1893 (2002)", International Research Journal of Engineering and Technology (IRJET), ISSN: 2395-0056, VOLUME: 02.

[71] D. M. Daniel and S. T. John (2016), "Pushover Analysis of RC Building", International Journal of Scientific & Engineering Research (IJSR), ISSN 2229-5518, Vol. 7.

[72] S. Sangeetha and A. Sathyapyiya (2017), "Pushover analysis for seismic assessment of RC building", International Research Journal of Engineering and Technology (IRJET), e-ISSN: 2395 -0056, Volume: 04.

[73] N. Ning, D. Yu, C. Zhang and S. Jiang, (2017), "Pushover Analysis on Infill Effects on the Failure Pattern of Reinforced Concrete Frames", MDPI, Appl. Sci. 2017, 7, 428; DOI: 10.3390/app7040428.

[74] O. Cavdar, A. Cavdar and E. Bayraktar (2017), "Earthquake Performance of Reinforced-Concrete Shear-Wall Structure Using Nonlinear Methods", Journal of Performance of Constructed Facilities. 32(1):04017122.

[75] S. A. Al-jassim and M. Husssain (2018), "Pushover Analysis of G+5 Reinforced Concrete Building in Basrah", International Journal of Innovations in Engineering and Technology (IJIET), ISSN: 2319-1058, Volume.

[76] D. Abhilash and M. Vijayanand (2019), "Pushover Analysis of a Multi-Storied Building in Two Different Zones", International Journal of Innovative Research in Science, Engineering and Technology, ISSN (Online): 2319-8753, Vol. 8.

[77] N. V. Ingale and L .G. Kalurkar, (2020), "Study the Effect of Push Over Analysis for G+15 Story R.C Structure with and without Zipper Frame using Sap-2000", International Journal of Engineering Research & Technology (IJERT) ISSN: 2278-0181, Vol. 9.

[78] R. Ayre (1938) "Interconnection of translational and torsional vibration in structures", Bull Seism Soc Am 28:89–130.

[79] G. P. Cimellaro, A. M. Asce, T. Giovine and, D. G. Lopez (2014), "Bidirectional Pushover Analysis of Irregular Structures", Journal of Structural Engineering, ©SCE, ISSN 0733-9445/04014059(13).

[80] M. Mohod (2015), "Pushover Analysis of Structures with Plan Irregularity", IOSR Journal of Mechanical and Civil Engineering (IOSR-JMCE), -ISSN: 2320-334X, Volume 12, Issue 4.

[81] P. Fajfar, Y. Marus and I. Perus, (2005b), "The extension of N2 method to asymmetric buildings", Proceedings of the 4th European workshop on the seismic behavior of irregular and complex structures, Thessaloniki, Greece.

[82] A. Chopra and R. Goel (2004), "A modal pushover analysis procedure for estimating seismic demands for unsymmetric-plan buildings". Earthq Eng Eng Vib 33:903–927.

[83] M. ,Jianmeng, Z. Changhai and X. Lili, (2008), "An improved modal pushover analysis procedure for estimating seismic demands of structures", Earthq Eng & Eng Vib (2008) 7:25-31, Vol.7, No.1.

[84] M. Kreslin and P. Fajfar (2011) "The extended N2 method taking into account higher mode effects in elevation", Journal of Earthquake Engg. Struct.Dyn, 40, 1571-1589.

[85] D. Menachery, and N. Manjula (2014), "Application of Extended N2 Method to Reinforced Concrete Frames with Asymmetric Setbacks", International Journal of Civil Engineering and Technology (IJCIET), ISSN 0976, Volume 5, Issue 12, pp. 143-154.

[86] American Society of Civil Engineering (ASCE 7-10) (2010) Minimum design loads for buildings and other structures. American Society of Civil Engineers, Reston, VA.

[87] Turkey Building Earthquake Code 2018, Ankara, Turkey.

[88] M. Zameeruddin, , M. Saleemuddin, and K. Sangle, (2017), "Seismic Damage Assessment of Reinforced Concrete Structure using Non-linear Static Analyses", KSCE Journal of Civil Engineering, ISSN 1226-7988,

[89] M. Inel, and H. B. Ozmen (2006), "Effects of plastic hinge properties in nonlinear analysis of reinforced concrete buildings", ELSEVIER, Engineering Structures 1494–1502.

[90] A. A. Eslami and H. R. Ronagh(2014), "Effect of elaborate plastic hinge definition on the pushover analysis of reinforced concrete buildings", Ph.D., dissertation to, School of Civil Engineering, The University of Queensland, Brisbane, QLD, 4072, Australia.

[91] Y. Jadhavand and V. Patil (2017), "Effect of User Defined Plastic Hinges on Nonlinear Modeling of Reinforced Concrete Frame for Seismic", International Research Journal of Engineering and Technology (IRJET), ISSN: 2395-0056, Volume: 04.

[92] A. L. LÓPEZ, A. ESPÍN and G. S. OLIVARES, (2017), "Seismic behavior of concrete structures depending on the model of plastic hinge", VII Congreso Internacional de Estructuras de ACHE, A Coruña, Spain.

[93] "Manual on Seismic Evaluation and Retrofit of Multi-storeyed RC Buildings", Sponsored by Department of Science and Technology Government of India

[94] G. Occhipinti, (2017), "Seismic Assessment and Rehabilitation of Existing RC Buildings not designed to withstand earthquakes", Ph.D., dissertation to Department of Civil and Environmental Engineering University of Catania.

[95] C. Durucan, and M. Dicleli, (2010), "Analytical study on seismic retrofitting of reinforced concrete buildings using steel braces with shear link", Engineering Structures, vol. 32, pp. 2995-3010, 2010.

[96] H. Fahmi and F. Faraj "Seismic evaluation of

existing reinforced concrete buildings", Eng & Technology, Vol.19, No.1, 5-3-1998.

[97] S. Dhiman, N. Mohammed and I. Nazrul (2015), "Behavior of Multi-storey RCC Structure with Different Type of Bracing System (A Software Approach)", International Research Journal of Engineering and Technology (IRJET), ISSN (Online) 2319-183X, Volume 4, PP.70-82.

[98] N. Bhojkar, and M. Bagade, (2015), "Seismic Evaluation of High-rise Structure by Using Steel Bracing System", International Journal of Engineering Trends and Technology (IJETT), Vol.47 No.5

[99] Bentley, "OpenSTAAD V8i (SELECT series 4) Reference manual," 2012. Available: http://www.bentley.com.

[100] M. Hyderuddin, M. Imran, and S. Mohsin(2016), "Retrofitting of Reinforced Concrete Frames using Steel Bracing", IJSRD - International Journal for Scientific Research & Development| Vol. 4, ISSN (online): 2321-0613.

[101] S. Basereh, P. Okumus, and S. Aaleti, (2020), "Seismic Retrofit of Reinforced Concrete Shear Walls to Ensure Reparability", ASCE, Structures Congress.